J. Fluid Mech. (1985), *vol.* 159, *pp.* 379–407
Printed in Great Britain

Evolution of scalar spectra with the decay of turbulence in a stratified fluid

By A. E. GARGETT

Institute of Ocean Sciences, 9860 West Saanich Road, Sidney, B.C., Canada V8L 4B2

(Received 24 October 1984 and in revised form 19 April 1985)

Temperature measurements taken in association with the velocity measurements described by Gargett, Osborn & Nasmyth (1984) are examined. With careful noise removal the temperature dissipation spectrum is fully resolved and χ, the dissipation rate of temperature-fluctuation variance, is determined directly. With directly measured values of χ and ϵ, the turbulent-kinetic-energy dissipation rate per unit mass, the observed temperature spectra are non-dimensionalized by Oboukov–Corrsin–Batchelor scaling. Shapes and levels of the resulting non-dimensional spectra are then examined as functions of the degree of isotropy (measured) in the underlying velocity field. Two limiting cases are identified: Class A, associated with isotropic velocity fields; and Class B, associated with velocity fields which are anisotropic (owing to buoyancy forces repressing vertical relative to horizontal dimensions of energy-containing 'eddies'). The present observations suggest that the Corrsin–Oboukov–Batchelor theory does not provide a universal description of the spectrum of temperature fluctuations in water. Class A scalar spectra have neither $k^{-\frac{5}{3}}$ nor k^{-1} subranges: a Batchelor-spectrum fit to the high-wavenumber roll-off region yields a value of 12 for the 'universal' constant q. In striking contrast, the buoyancy-affected Class B spectra exhibit a clear $k^{-\frac{5}{3}}$ subrange, an approach to a k^{-1} subrange, and a value of $q \sim 4$ which is in rough agreement with most previous estimates. Previous oceanic and atmospheric measurements are re-examined in the light of the present results. It is suggested that these previous results are also affected by vertical scale limitation. Reasons underlying the discrepancies between theories and observations are discussed: these may be different in the two classes presented.

1. Introduction

This paper is a companion to that of Gargett, Osborn & Nasmyth (1984, hereinafter referred to as GON) which described observations of turbulent velocity fields associated with various instabilities of tidal flows in Knight Inlet, British Columbia. Simultaneous measurements of the temperature field are described here and compared with theories available for the spectrum of a passive scalar in a fluid of moderate Prandtl number.

A passive scalar is a fluid property which is merely advected by a fluid flow without affecting the dynamics of that flow: thus any theory of scalar-variance distribution depends upon some underlying model of the advecting flow. For a turbulent flow, this underlying model is invariably that of Kolmogoroff (1941) (see Monin & Yaglom 1975; also GON): here, only relations necessary for discussion of the temperature data will be reviewed. Briefly, Kolmogoroff proposed that for sufficiently large Reynolds number Re there would be found a range of wavenumbers within which the turbulent velocity field is isotropic and dependent only upon the molecular viscosity ν and the

rate ϵ at which kinetic energy was being transferred to dissipation scales. Thus, defining the one-dimensional energy spectrum $\phi_{11}(k)$ such that

$$\overline{u_1^2} \equiv \int_0^\infty \phi_{11}(k)\,\mathrm{d}k,$$

with k the (radian) wavenumber in the direction of the streamwise velocity component u_1:

$$\phi_{11}(k) = \epsilon^{\frac{2}{3}} k^{-\frac{5}{3}} F\left(\frac{k}{k_s}\right), \tag{1}$$

where $F(k/k_s)$ is a universal function, $k_s \equiv (\epsilon/\nu^3)^{\frac{1}{4}}$ is the Kolmogoroff wavenumber and

$$\epsilon = 15\nu \int_0^\infty k^2 \phi_{11}(k)\,\mathrm{d}k \tag{2}$$

is the kinetic-energy dissipation rate per unit mass. If there exists a part of this range in which ν is not important, then the spectrum has an inertial subrange

$$\phi_{11}(k) = A_1 \epsilon^{\frac{2}{3}} k^{-\frac{5}{3}}, \tag{3}$$

where A_1 is a universal constant. Using the isotropic relations between axial ($\phi_{11}(k)$) and cross-component ($\phi_{jj}(k)$, $j = 2, 3$) spectra

$$\phi_{jj}(k) = \frac{1}{2}\left[\phi_{11}(k) - k\,\frac{\partial \phi_{11}(k)}{\partial k}\right], \tag{4}$$

one finds that in an inertial subrange

$$\phi_{jj}(k) = A_2 \epsilon^{\frac{2}{3}} k^{-\frac{5}{3}} \quad \text{with } A_2 = \tfrac{4}{3} A_1. \tag{5}$$

Oboukov (1962) and Kolmogoroff (1962) later revised this theory to allow for observed intermittency in the dissipation rate ϵ, which was found to be an increasing function of turbulent Reynolds number $Re_\lambda \equiv (\overline{u^2})^{\frac{1}{2}} \lambda/\nu$, where $\lambda \equiv (\overline{u^2}/\overline{(\partial u/\partial x)^2})^{\frac{1}{2}}$ is the Taylor microscale. However, reasonable approximations to the distribution of ϵ suggest that the variation in second-order quantities such as the spectrum should be very weak (Grant, Stewart & Moilliet 1962; Yaglom 1966; Antonia & Van Atta 1975).

For a passive scalar advected by such a turbulent field, if θ is the deviation of a scalar property from its ensemble mean, then

$$\overline{\theta^2} = \int_0^\infty \Gamma(k')\,\mathrm{d}k' = \int_0^\infty \psi(k)\,\mathrm{d}k, \tag{6}$$

where $\Gamma(k')$ is the three-dimensional, and $\psi(k)$ the one-dimensional, scalar spectrum. For isotropic turbulence, these are related by

$$\Gamma(k) = -k\,\frac{\partial \psi(k)}{\partial k} \tag{7}$$

and χ, the mean rate of dissipation of scalar variance $\overline{\theta^2}$, is given by

$$\chi = 6D \int_0^\infty k^2 \psi(k)\,\mathrm{d}k, \tag{8}$$

where D is the molecular diffusivity of the scalar.† The form of $\psi(k)$ within a velocity

† Definitions of ψ, hence χ, may differ among authors, depending upon whether the scalar budget is written for $\overline{\theta^2}$ (as here) or $\frac{1}{2}\overline{\theta^2}$: any intercomparison of experimental results must be corrected for this difference (Paquin & Pond 1971).

inertial subrange, obtained from dimensional arguments similar to those used by Kolmogoroff, is

$$\psi(k) = B\epsilon^{-\frac{1}{3}}\chi k^{-\frac{5}{3}}, \tag{9}$$

with B another universal constant (Oboukov 1949; Corrsin 1951). This is called the inertial–convective scalar subrange.

For a case such as that of temperature in water, which has a Prandtl number $Pr = \nu/D > 1$, theory relevant to the scalar spectral shape for wavenumbers above the inertial subrange was developed by Batchelor (1959). Briefly, Batchelor argued that the rate of strain $\gamma \sim (\epsilon/\nu)^{\frac{1}{2}}$ of the velocity field is approximately uniform over regions of linear dimensions small compared to k_s^{-1} (this is of course because the variance of velocity shear (rate of strain) resides near the peak of the velocity-dissipation spectrum, at wavenumbers less than k_s). For a fluid of $Pr \gg 1$ there then exists a range of wavenumbers which are larger than k_s but smaller than those wavenumbers at which thermal diffusion becomes important, characteristically a wavenumber

$$k_B \equiv \left(\frac{\epsilon}{\nu D^2}\right)^{\frac{1}{4}} = Pr^{\frac{1}{2}} k_s \tag{10}$$

which has become known as the Batchelor wavenumber. In this wavenumber range, $k_s \lesssim k \lesssim k_B$, a scalar-variance spectrum $\psi \propto k^{-1}$ results from extension of constant-scalar surfaces by the least principal rate of strain

$$\gamma \equiv -\frac{1}{q}\left(\frac{\epsilon}{\nu}\right)^{\frac{1}{2}}, \quad q = \text{constant}, \tag{11}$$

a process which delivers scalar variance to temperature-dissipation scales at rate χ. Dimensional consistency then requires

$$\psi(k) = q\frac{\chi}{\gamma}k^{-1}, \tag{12}$$

the so-called viscous–convective subrange of Batchelor. Expressions (9) and (12) may be combined to solve for k_*, the wavenumber of the intersection of inertial and viscous–convective subranges, in terms of the universal constants B and q and the Kolmogoroff wavenumber k_s. Hence

$$\frac{k_*}{k_s} = \left(\frac{B}{2q}\right)^{\frac{3}{2}} > 1, \tag{13}$$

where the inequality arises through the conditions associated with Batchelor's physical model of the viscous–convective subrange. Batchelor (1959) also derived a more complete form, including the diffusive roll-off,

$$\Gamma(k) = -\frac{\chi}{\gamma}k^{-1}\exp\left[\frac{D}{\gamma}k^2\right] \tag{14}$$

for the three-dimensional spectrum at wavenumbers $k > k_*$. The one-dimensional form of this spectrum (Gibson & Schwarz 1963) is given by

$$\psi(k) = 2\pi^{\frac{1}{2}}q^{\frac{3}{2}}D^{\frac{1}{2}}\left(\frac{\nu}{\epsilon}\right)^{\frac{3}{4}}\left[\frac{N(b)}{b} - \int_0^\infty N(y)\,dy\right], \tag{15}$$

where

$$N(b) = (2\pi)^{\frac{1}{2}}\exp(-\tfrac{1}{2}b^2) \quad \text{and} \quad b = (2q)^{\frac{1}{2}}k/k_B.$$

The study of intermittency effects on the scalar spectrum was begun by Kraichnan (1968). Batchelor's model (11) is that of a rate of strain γ which is statistically sharp in amplitude but which has random directions over scales large compared to k_s^{-1}. Kraichnan used a simple example of a strain-rate distribution random in *both* amplitude and direction to demonstrate that, for a high-Prandtl-number fluid, the k^{-1} subrange still emerges and the functional form of the diffusive roll-off survives. However, in the expression (11) for γ the 'constant' q increases with increasing intermittency.

Van Atta (1971, 1973) investigated the influence of intermittency in *both* ϵ (hence γ) and χ on the inertial subrange of the scalar spectrum for the case $Pr \geqslant 1$. He assumed that the distributions of ϵ_r and χ_r, values of ϵ and χ averaged over a volume of radius r, are both lognormal with equal variances $\sigma^2_{\ln \epsilon_r} = \sigma^2_{\ln \chi_r} = A + \mu \ln (L/r)$, where L is some outer scale of the turbulence, and that their joint distribution is bivariate lognormal. The resulting slope m of the scalar inertial subrange was found to depend upon the parameter μ and the correlation coefficient $\rho(r)$ between ϵ_r and χ_r as

$$m = -\tfrac{5}{3} + \tfrac{1}{3}\mu(\tfrac{2}{3} - \rho(r)). \tag{16}$$

Arguing that $|\rho(r)| \leqslant 1$ can be at most a weakly varying function of r, and using an experimentally determined value of $\mu \simeq 0.5$ (Wyngaard & Pao 1971; Gibson, Stegen & McConnell 1970) Van Atta found that the slope m ranges from -1.39 for $\rho = -1$, through the classical value of $-\frac{5}{3} = -1.67$ for $\rho = +\frac{2}{3}$, to -1.72 for $\rho = +1$. The assumed distribution of ϵ_r and χ_r also modifies the value of the 'universal' constant B to

$$B' = B \exp\left[\tfrac{1}{3}A(\tfrac{2}{3} - \rho)\right]. \tag{17}$$

With $A \sim O(1)$ (Antonia & Van Atta 1975), B' ranges from $1.74B$ for $\rho = -1$ to $0.89B$ for $\rho = +1$.

Unfortunately, the approach used by Van Atta is not readily extended to obtain the scalar spectrum at wavenumbers beyond the inertial subrange (Antonia & Van Atta 1975); hence we are left without a comprehensive picture of the effect of intermittency for the case $Pr > 1$.

The available observational evidence for the Kolmogoroff theory of the velocity spectrum will not be reviewed in any detail here (see Monin & Yaglom 1975; Williams & Paulson 1977; Mestayer 1982). In high-Reynolds-number turbulence, axial velocity spectra do exhibit an 'inertial' subrange ((3)), with an apparently universal value of $A_1 \sim 0.55$. However, it has long been noticed, in association with the atmospheric-boundary-layer measurements which form the bulk of available observations, that the $-\frac{5}{3}$ subrange in $\phi_{11}(k)$ extends to wavenumbers which are far lower than those which may reasonably be expected to be isotropic (i.e. far lower than $O(z^{-1})$, where z is the distance of the sensors from the boundary). The very few studies which are able to check more stringent requirements of isotropy, such as (4) or (5), often find that these are not satisfied for wavenumbers within the $-\frac{5}{3}$ subrange of the $\phi_{11}(k)$ spectrum (Weiler & Burling 1967; Mestayer 1982). The degree to which the turbulent velocity fields observed in Knight Inlet fulfil major requirements of Kolmogoroff's theory varies considerably: the results of GON will be briefly reviewed in §3 to provide a framework for discussion of the associated temperature measurements.

Experimental evidence of the universal nature of the passive-scalar spectrum in an inertial subrange is considerably more scattered than the velocity spectral

measurements. Temperature spectral subranges with $-\frac{5}{3}$ slope have frequently been observed, but values of the 'universal' constant B range from 0.35 (Gibson & Schwarz 1963) to 1.15 (Gibson, Stegen & Williams 1970). As will become clear, much of this scatter may be attributed to experiments in which χ had to be determined indirectly by curve-fitting to the low-wavenumber end of the observed spectrum. Eliminating such experiments leaves only three studies, all in the atmospheric boundary layer, which can be used to assess the universality of the inertial-convective subrange. Boston & Burling (1972) measured u_1 and T at 4 m above a tidal mud flat during daytime-heating conditions, and estimated $B = 0.81$. Champagne *et al.* (1977) made the same measurements over a flat ploughed field and obtained $B = 0.45$. Measuring the same quantities at 2 m over a nearly level field of harvested rye grass, Williams & Paulson (1977) determined $B = 0.50$ on average, but suggested that B was an increasing function of Re_λ. These results will be discussed further in §6.

The main purpose of the present study is to describe the spectrum of temperature in seawater ($Pr \simeq 7$) in a case where all three components of the velocity field, as well as the temperature field, were resolved through dissipation scales. The setting of the measurements is reviewed briefly in §2, followed (§3) by a short summary of the associated velocity fields: further details may be found in GON. A description of the temperature-measurement technique is found in §4 and the Appendix, along with a discussion of error in the estimates of ϵ, χ and buoyancy frequency $N \equiv -g\rho_0^{-1}\,\partial\rho/\partial z$, this last an essential parameter for stratified flows. In §5 observed temperature spectra are examined in the light of the theoretical framework outlined above. Section 6 discusses various possible reasons for the inadequacy of this framework.

2. Setting of measurements

Measurements were taken on 16–21 November 1978 from the research submersible PISCES IV operating in Knight Inlet. A fjord on the mainland coast of British Columbia, Knight Inlet is divided into two basins by a 60 m-deep sill over which semi-diurnal tides move a water column strongly stratified by freshwater input to the surface layer. At the time of observations, the buoyancy frequency N ranged from ~ 0.01 rad s^{-1} (~ 6 c.p.h.) at a depth of ~ 30 m to values in excess of 0.03 rad s^{-1} (~ 20 c.p.h.) very near the surface. Despite the strong (by oceanic standards) stratification, tidal energy is often sufficient to generate turbulence through any of a variety of internal hydraulic mechanisms (Farmer & Smith 1980).

In November 1978 ebb-tidal flows produced a stationary lee wavetrain and a turbulent separated boundary layer downstream of the sill, both seen in the 200 kHz echo-sounder record of figure 1(*c*). The path of submersible measurements on November 21 (data tapes 837–839) in the far field of the separated boundary layer is shown to the west of the sill in the map of figure 1(*a*): no measurements were taken in the stronger turbulence near the sill owing to the danger of running probes (and submersible) into the ridge. As the tidal flow reversed to flood, the lee wavetrain separated from the sill and moved up-inlet ($\sim$ east). As it propagated, the leading waves increased in amplitude and eventually developed intense turbulence in their troughs, while additional waves formed and grew behind them. The echo-sounding of figure 1 (*b*) shows such a wave group as observed with its leading edge in the vicinity of Station 5 in figure 1(*a*). Measurements were taken through various parts of the flood-tide wavetrain on several consecutive days. Approximate dive tracks are shown in figure 1(*a*), identified by date. This report uses data from dives on 15 November

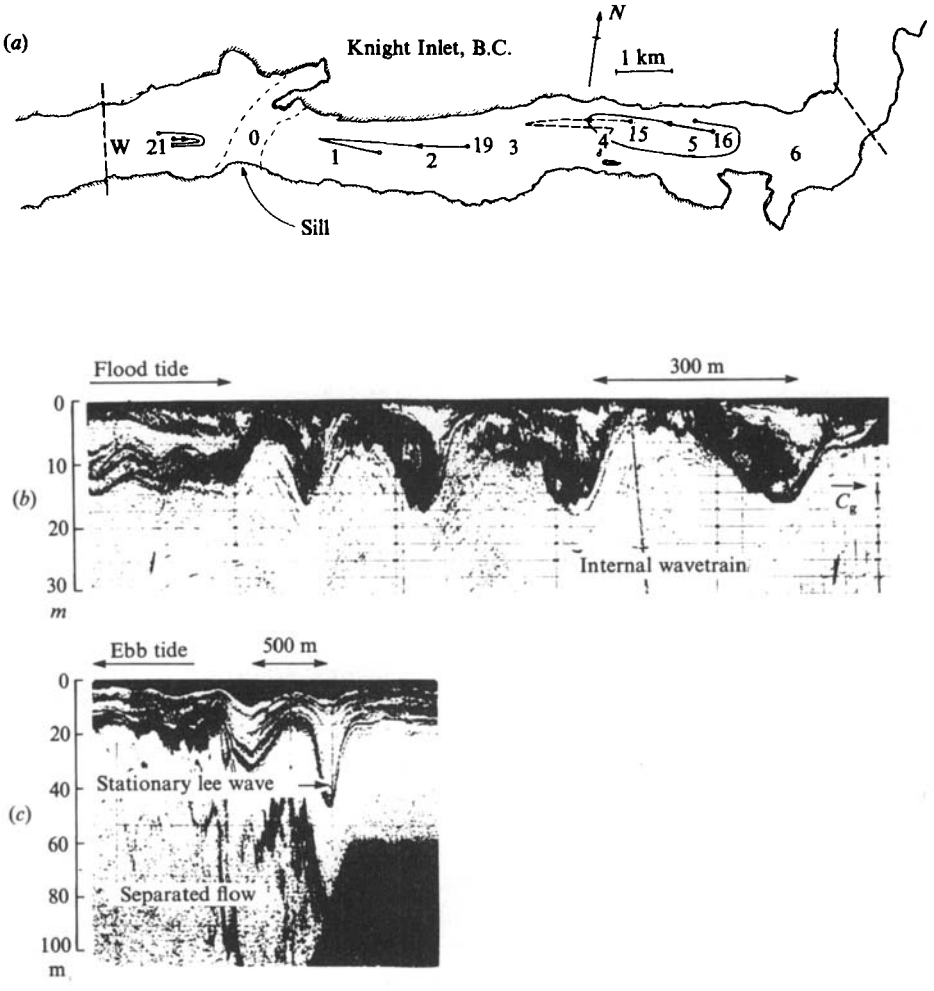

FIGURE 1 (from Gargett, Osborn & Nasmyth 1984). (*a*) Plan section of a portion of Knight Inlet, showing the location of the sill which divides the inlet into two basins. Turbulence measurements were taken from the submersible PISCES IV during the week of 15–22 November 1978. Submersible tracks are identified by date. Marked stations (W and 0–5) are locations of CTD profiles. (*b*, *c*) The two flow regimes in which measurements were taken are shown here (courtesy of David Farmer) in records from a 200 kHz echo-sounder operated during the week of turbulence measurements (horizontal scales are approximate): (*b*) measurements east of the sill were taken in an internal wavetrain released from the sill on the turn to flood tide; (*c*) to the west of the sill, measurements were taken in separated flow which occurs downstream of the sill on ebb tide.

(data tape 822) through the leading waves, 16 November (data tapes 823–825) through the leading waves and the undisturbed waters up-inlet of the wave group, and 19 November (data tape 831) in the far field of the wavetrain.

Measurements are referred to a coordinate system x_i ($i = 1, 2, 3$) attached to the submersible, a (moving) geographic coordinate system with x_1 taken in the direction of travel and x_3 vertically upwards (GON, figure 4 and §3.2). High-frequency velocities were measured by a heated-film probe (u_1) and two orthogonal airfoil probes (u_2, u_3), low-frequency velocity components U_i ($i = 1, 2, 3$) by a triplet of small ducted rotors. High-frequency temperature T' was sensed by a cold-film probe and low-

frequency temperature T by a thermistor. Auxiliary sensors included a second thermistor T_B for temperature difference $T_B - T = \Delta T$ over 0.8 m vertically, a pressure gauge, and three accelerometers. A complete description of the combined sensor–vehicle system is found in Gargett (1981) while analog traces of the data collected on PISCES are shown in figures 5 (*a*) and 5 (*b*) of GON for many of the records used in this paper.

3. The velocity field

While the theory of Kolmogoroff was proposed for turbulence in a homogeneous environment, it may be expected to apply to stratified systems provided attention is restricted to scales smaller than the scale at which stable stratification inhibits overturning. Since the buoyancy wavenumber $k_b \equiv (N^3/\epsilon)^{\frac{1}{2}}$ has long been associated with such a maximum overturning scale (Dougherty 1961; Ozmidov 1965) GON attempted to classify the velocity spectra measured in Knight Inlet as a function of the parameter $I \equiv k_b/k_s$. This isotropy parameter, a measure of the separation between energy-containing and dissipation scales in a stratified fluid (hence the amount of 'room' in wavenumber space for development of an inertial subrange), worked well as a basis for classification. The highest observed values of $I \sim O(3000)$ were associated with velocity spectra which all exhibited distinct $-\frac{5}{3}$-subranges and in addition satisfied relation (4) over most of the range of observed wavenumbers. In this paper these will be called Class A spectra: the $+\frac{5}{3}$-moment spectra of the axial component (ϕ_{11}) and the vertical cross-component (ϕ_{33}) are shown in figure 2, averaged over the five Class A records used in subsequent discussion. The spectra are plotted in the non-dimensional form $\hat{\phi} \equiv \phi/(\epsilon\nu^5)^{\frac{1}{4}}$ as a function of non-dimensional wavenumber $\hat{k} \equiv k/k_s$, where $k_s = (\epsilon/\nu^3)^{\frac{1}{4}}$ is calculated using the record-averaged value of ϵ (table 1). Levels corresponding to values of 0.55 and 0.60 for the Kolmogoroff constant A_1 are shown on both spectra. These Class A spectra have an inertial subrange, in the sense of relation (5), over the range $-2.4 \lesssim \log \hat{k} \lesssim -1$ before rolling off with universal shapes at dissipation scales.

As measured I decreases, the ϕ_{11} spectrum maintains a $k^{-\frac{5}{3}}$ subrange and the universal level of the Class A spectra, while both cross-component spectra develop a distinct k^{-1} subrange. This k^{-1} subrange is not universal, in a Kolmogoroff sense, in either level or extent. Rather, it is associated with the fact that the fluid is stratified, since it collapses to a constant level when non-dimensionalized with buoyant-turbulence parameters k_b and $u_b \equiv (\epsilon/N)^{\frac{1}{2}}$ (see GON, §6). The high-wavenumber end of the k^{-1} range occurs at $k \simeq 10k_b$. At the higher wavenumbers typical of the velocity-dissipation scales the velocity spectra continue to achieve the universal Kolmogoroff shapes and to satisfy relation (4).

By the lowest measured values of $I \sim 50$–100 (Class B spectra), even the ϕ_{11} spectrum finally begins to fall below the universal curve, most seriously at the lowest wavenumbers. The k^{-1} range of ϕ_{33} now covers at least the decade between $-2 < \log \hat{k} < -1$ (at lower wavenumbers the measurements fall to the system noise level). Class-averaged values of Class B velocity spectra are also shown in figure 2. Note that, within the variance error limits, scales contributing substantially to the dissipation (i.e. within the decade below $\log \hat{k} = 0$) still follow universal curves when normalized by Kolmogoroff scales.

It should be noted that the Class B spectra represent a limit of measurement technique, not necessarily of the turbulent spectral shapes. However, further increase of anisotropy within the dissipation range will affect ability to estimate the

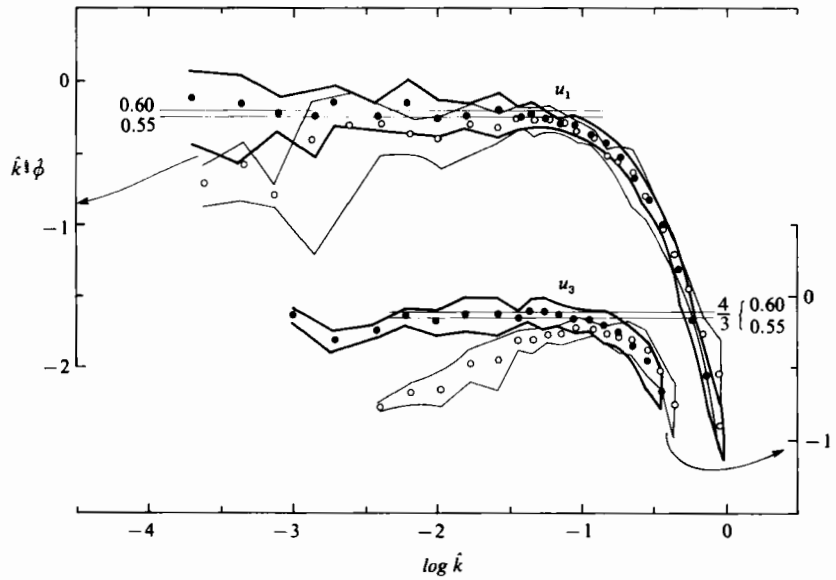

FIGURE 2. Axial (u_1) and vertical (u_3) cross-component spectra are non-dimensionalized by the Kolmogoroff scaling $\hat{\phi} = \phi/(\epsilon\nu^5)^{\frac{1}{4}}$ and plotted here as the $+\frac{5}{3}$-moment spectrum $\hat{k}^{\frac{5}{3}}\hat{\phi}$ as a function of $\hat{k} = k/k_s$, where $k_s = (\epsilon/\nu^3)^{\frac{1}{4}}$ is the Kolmogoroff wavenumber. A flat region in this plot indicates an inertial ($k^{-\frac{5}{3}}$) subrange in the velocity spectrum. The solid and open circles are class-averaged values for records termed Class A and B, respectively, each class consisting of five independent records of varying length. Variance error bars are shown as solid and light lines respectively. Class A records are characterized by inertial subranges in both component spectra, with a value of the Kolmogoroff constant A between 0.55 and 0.60 (levels indicated). The Class B records maintain an 'inertial' subrange in the u_1 spectrum, but the vertical velocity spectrum now falls approximately as $\hat{k}^{-1}$ ($\hat{k}^{+\frac{5}{3}}$ in this representation) over at least a decade before the diffusive rolloff at the highest wavenumbers.

fundamental parameter ϵ from a single velocity-component measurement, hence make it difficult to test for any continuing degree of universality during further decay of the velocity field.

Two other results will be used in subsequent discussions. First, GON found that for those velocity fields which showed evidence of the influence of buoyancy, including of course the Class B records, a typical velocity variance was $(\overline{u_1^2}) \simeq u_b^2 = \epsilon/N$. For the Class A spectra it was not possible to estimate $(\overline{u_1^2})$ directly from measurements: extrapolating the measured spectral slope back to $k \sim \frac{1}{2}k_b$ (as used for the direct calculations of the buoyancy-affected records) gave $(\overline{u_1^2}) \sim (2\text{–}3)\,u_b^2$. For Class A records the cross-component variances $\overline{u_2^2} \sim \overline{u_3^2} \sim \overline{u_1^2}$, while for Class B records $\overline{u_2^2} \sim \overline{u_1^2}$ and $\overline{u_3^2} \sim 0.6\overline{u_1^2}$. Secondly, a vertical overturning scale of $l_0 \sim \frac{1}{3}l_b$, where $l_b \equiv 2\pi/k_b$, was estimated from a number of constraints on the observational data. It was argued that this value of l_0 is consistent with other recent results from the laboratory (Stillinger, Helland & Van Atta 1983) and the ocean (Gargett *et al.* 1981). Crawford (1985) has recently demonstrated that it is also consistent with the oceanic results of Dillon (1982).

Record	ϵ $m^2\,s^{-3}$	χ $(°C)^2\,s^{-1}$	N rad s^{-1}	k_s rad m^{-1}	I	Re_λ	Cx	Γ
Class A								
▽ 822-1-1030-74	$2.8\,10^{-5}$	$1.3\,10^{-5}$ (10)	—	1740	—	—	—	—
□ 822-1-2975-126	$9.9\,10^{-6}$	$9.1\,10^{-7}$ (30)	—	1300	—	—	—	—
○ 825-2-2350-48	$1.8\,10^{-5}$	$4.5\,10^{-6}$ (16)	$1.9\,10^{-2}$	1500	2500	(2–3) × 710	$2.4\,10^4$	0.21
● 825-2-2725-73	$2.1\,10^{-5}$	$4.2\,10^{-6}$ (8)	$1.6\,10^{-2}$	1600	3600	(2–3) × 910	$5.0\,10^4$	0.25
▲ 825-2-3150-40	$3.8\,10^{-5}$	$6.0\,10^{-6}$ (21)	$2.0\,10^{-2}$	1900	4000	(2–3) × 980	$2.5\,10^4$	0.12
Class B								
○ 831-1-3925-163	$1.3\,10^{-6}$	$2.5\,10^{-6}$ (2)	$2.2\,10^{-2}$	800	270	170	$2.0\,10^3$	0.31
● 831-2-400-122	$2.2\,10^{-7}$	$4.7\,10^{-7}$ (14)	$2.2\,10^{-2}$	490	70	70	$4.0\,10^2$	0.34
□ 831-2-2355-11	$4.1\,10^{-6}$	$2.1\,10^{-5}$ (16)	$4.2\,10^{-2}$	740	190	160	$1.3\,10^3$	0.23
△ 837-2-4100-61	$9.7\,10^{-7}$	$2.5\,10^{-6}$ (16)	$2.4\,10^{-2}$	1100	250	130	$1.4\,10^3$	0.35
▼ 839-1-700-126	$2.6\,10^{-8}$	$6.6\,10^{-8}$ (18)	$1.9\,10^{-2}$	300	20	30	$8.2\,10^1$	0.41

TABLE 1. Parameters associated with individual records, grouped by class (the symbol to the left of the record identification is that used in figure 5). Records are identified by Tape number – File number – Starting record number – M, where M is the number of Fourier blocks averaged ($M/0.976$ = record length in metres). The fundamental scaling parameters ϵ, χ and N are derived from measurements, as described in the text, §§3 and 4. $k_s \equiv (\epsilon/\nu^3)^{\frac{1}{4}}$ is the Kolmogoroff wavenumber ($\nu = 1.48 \times 10^{-6}\ m^2\,s^{-1}$). The isotropy ratio $I \equiv k_s/k_b$, where $k_b \equiv (N^3/\epsilon)^{\frac{1}{2}}$ is the buoyancy wavenumber. Re_λ is the turbulent Reynolds number (§1), calculated with $\langle u^2 \rangle \sim u_b^2 \equiv \epsilon/N$ (the factor of 2–3 in the Class A records is an estimate only (§3); the (implicit) factor of 1 in the Class B records is better determined). The Cox number is here defined as $Cx \equiv \overline{(\partial T/\partial x)^2}/(\partial \overline{T}/\partial z)^2$ and calculated (with the assumption of temperature dissipation-scale isotropy) as $Cx = \chi/6D(\Delta T/\Delta z)^2$, using measured values of χ and $\Delta T/\Delta z$, with $D = 1.39 \times 10^{-7}\ m^2\,s^{-1}$. $\Gamma \equiv \zeta/\rho_0\epsilon$ is the ratio of the dissipation rate ζ of available potential energy to that of kinetic energy. ζ is estimated from the relation $\zeta = g\rho_0^2(\beta m^{-1} - \alpha)\,(\frac{1}{2}\chi)\,(|\Delta T/\Delta z|)^{-1}$, where g is the acceleration of gravity, ρ_0 is average seawater density, m is the local T/S slope, $\beta \equiv \rho_0^{-1}\partial\rho/\partial S$ and $\alpha \equiv -\rho_0^{-1}\partial\rho/\partial T$: the factor 2 enters because χ as used here is the dissipation rate of $\overline{(T')^2}$, while the dissipation rate of available potential energy is proportional to $\frac{1}{2}\overline{(T')^2}$. Note that this expression assumes that the T/S relation is scale-invariant.

4. Temperature-field measurements

The measured temperature spectrum is a composite of the output of an unheated platinum film probe at high frequencies and a thermistor (at the same level, approximately 0.2 m behind the cold film) at low frequencies. Details of the cold-film probe, circuit and calibration techniques for both gain and frequency response are given in the Appendix. Here I will discuss only the effective noise level of measured temperature spectra, and the errors in derived quantities such as χ, ϵ and N which are used to non-dimensionalize and/or classify results.

Temperature data selected for analysis had to satisfy a number of criteria. First, the associated velocity data had to be complete and of high quality (conditions given by GON, §3.4). In addition, chart records of velocity and temperature signals at frequencies above $\sim$ 1 Hz were examined to select fairly uniform stretches of record: no obvious changes in mean-square variances were allowed. This requirement was the fundamental limitation on record length. In a further attempt to select only samples which are as homogeneous as possible in an environment which was certainly inhomogeneous in large-scale temperature, I have used only records in which spectra from two thermistors 0.8 m vertically apart are statistically indistinguishable. The cold-film record is broken into blocks of 1024 points: with a 1000 Hz sample rate,

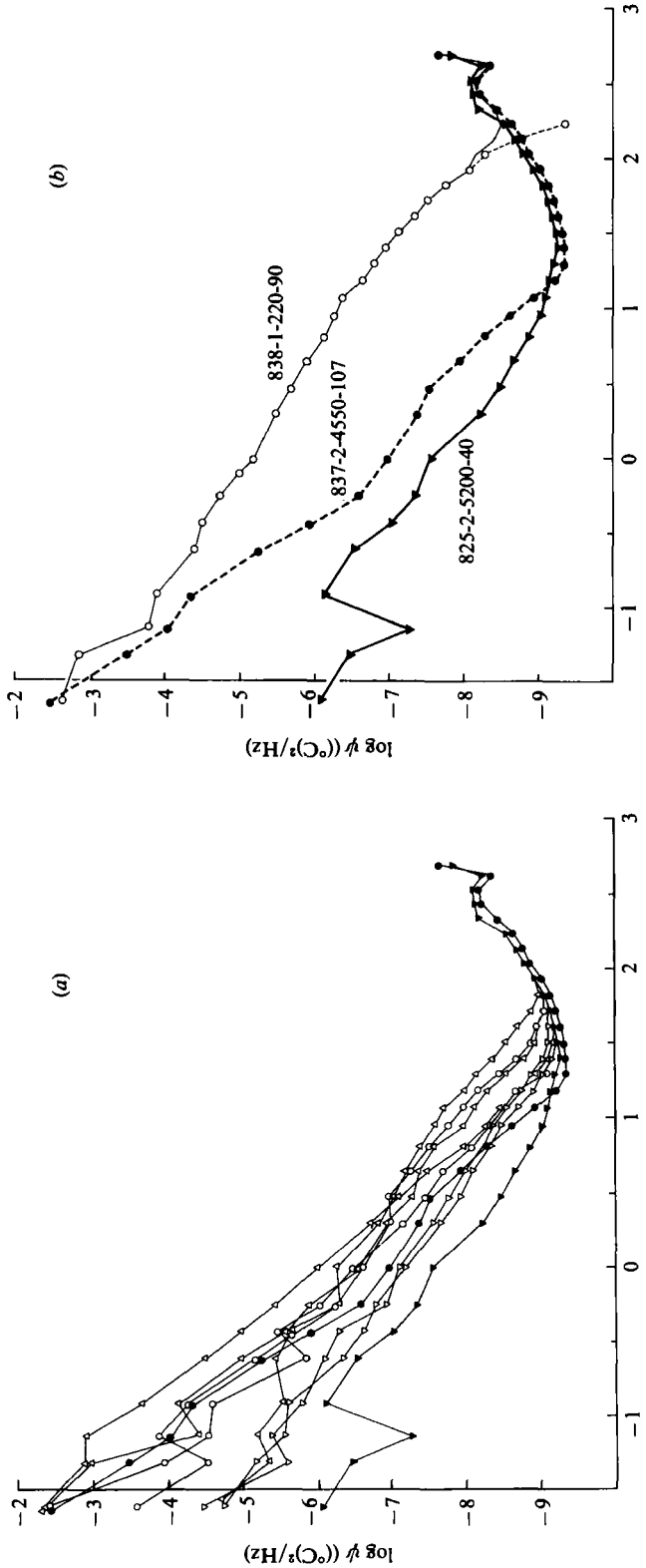

FIGURE 3. (*a*) Ensemble of noise-level temperature spectra from various dates and locations: ▽ denotes records taken on 16 November in the quiescent waters ahead of the internal wavetrain (▼ Record 825-2-5200-40 is the standard noise record chosen to correct observed temperature spectra); △ records taken on 19 November in the far field behind the internal wavetrain; and ○ records taken on 21 November in the separated boundary layer to the west of the sill (● Record 837-2-4550-107 is used to check sensitivity of χ to the choice of noise record). Spectra from both of these latter locations show residual temperature variance at low wavenumbers; however all spectra lie within very narrow bounds at the high frequencies where noise correction will most affect calculation of χ. (*b*) Correction of record 838-1-220-90 (light line) by subtraction of the standard noise record 825-2-5200-40 has substantial effect only at frequencies above 100 Hz, where the noise rises sharply: the light line shows the original spectrum, open circles the noise-corrected values. For this record, the noise spectrum 837-2-4550-107 taken on the same day might be more appropriate, but would substantially alter only the last couple of points retained in the corrected spectrum (see figure 4).

the spectrum is resolved to 0.976 Hz. The thermistor record, sampled at 25 Hz, is used to extend the spectrum to lower frequencies from a region of overlap between $f \sim 1$ Hz and 5 Hz. The lowest frequency used is $f_L \geqslant 2/T$, where T is the total available record length, so that the lowest-frequency estimate has a minimum of two degrees of freedom owing to block averaging. Each signal block is first-differenced and cosine-tapered (10%) before Fourier transforming, then resulting spectra are averaged over the number M of blocks available. The block-averaged spectrum is corrected for first-differencing and loss of variance owing to the cosine taper, then band-averaged in frequency with logarithmically increasing bandwidth. Corrections for system gains and (cold-film) response functions finally yield signal spectra. Each such record is identified by (Tape number – File number – Starting record number – M), where M is the number of degrees of freedom of the cold-film estimate at $f = 0.976$ Hz. Since the mean speed $\bar{U} \sim 1.0$ m s^{-1}, $(M/0.976) \approx$ record length in metres. The mean speed $\bar{U}$ is used to convert from frequency to wavenumber, invoking the frozen-field hypothesis of Taylor (see GON, §3.4).

A typical spectrum decreases with frequency, then starts to rolloff more rapidly before rising again at the highest frequencies recorded. This rise, due to electrical noise, shows very little change over an ensemble of 'noise-level' spectra (chosen as the lowest signal levels observed over the week of measurements), as can be seen in figure 3(*a*). In these records, the substantial variation apparent at low frequencies reflects differing environments: only 825-2-5200-40 comes from quiescent waters in front of the internal wavetrain: the remainder come from the far field of either the wavetrain (16 and 19 November) or the separated boundary layer (21 November), and hence contain residual signal variance. However, for $f > 100$ Hz, all these spectra lie within the narrow limits shown, suggesting that high-frequency-noise correction may be accomplished by subtracting a noise-level spectrum. An example of this technique, using 825-2-5200-40 as a standard noise spectrum, is shown in figure 3(*b*): corrected values (open circles) are generally non-zero to frequencies well beyond the peak of the temperature dissipation spectrum $k^2\psi$ (figure 4), which is integrated to provide an (isotropic) estimate of χ. For records taken on 21 November, when noise levels appear to be consistently lower than on 16 or 19 November (see record 837-2-4550-107 in figure 3(*a*), use of 825-2-5200-40 as a noise level will slightly underestimate χ (for the record 838-1-220-90 of figure 4, the difference is -7.6% in χ): it nevertheless seemed more conservative to remove consistently the highest observed noise level. A further correction to χ must be made because not all records resolve the entire dissipation range (although all records used in this paper clearly resolve the peak of the dissipation spectrum). This correction was done by extending an observed dissipation spectrum smoothly to zero, as shown by the dashed parts of the curves in figure 4, then determining the area under this completed curve. Maximum correction due to this effect was an increase of 30%; more typically, χ values were corrected by $\sim 15\%$. In table 1, a compilation of relevant parameters for all records used in this paper, the percent correction applied to χ owing to inadequate resolution is given in brackets behind the χ value.

The absolute accuracy of the χ-estimate obtained by using the measured variance $\overline{(\partial T'/\partial x)^2}$ in the isotropic formula (8) depends upon the accuracies of measured ψ at wavenumbers which contribute significantly to the gradient variance, of Taylor's hypothesis in high-intensity turbulence, and of the underlying assumption of isotropy. For the first, a maximum error of $\sim \pm 6\%$ may be expected, based on the estimated error associated with error in the cold-film response parameter Δ at frequencies near 500 Hz (see Appendix). The question of error associated with

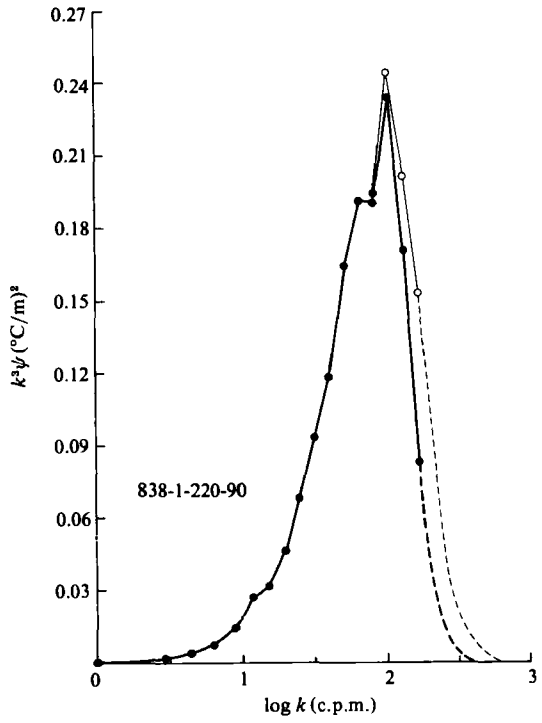

FIGURE 4. The maximum effect of noise-level choice on χ is illustrated in this variance-preserving plot of the temperature variance dissipation spectrum (χ is proportional to the area under this curve). Record 838-1-220-90 is shown corrected (dark circles) by the standard noise record 825-2-5200-40 and (open circles) by the alternate record 837-2-4550-107 which might be more appropriate: the resulting difference in χ is $\sim 7.6\,\%$. This figure also illustrates the extrapolation (dashed) used to complete the dissipation curve. The value of χ reported in table 1 is obtained by integration of the completed curve: the value in brackets after the χ value is the percentage of the value of χ which is associated with the area under the extrapolated portion of the dissipation curve.

Taylor's hypothesis was addressed by Champagne *et al.* (1977), who extended a model due to Heskestad (1965) to a scalar and concluded that χ is overestimated by a fraction

$$\left[\frac{\overline{u_1^2}+\overline{u_2^2}+\overline{u_3^2}}{(\bar{U})^2}\right]. \tag{18}$$

For the most highly turbulent (Class A) records, the energy-containing scales of the turbulence lie at scales comparable to or greater than the length of PISCES, so that the turbulent-velocity variances involved in (18) can only be estimated. One estimate (described in §3) uses $\overline{u_1^2} \sim \overline{u_2^2} \sim u_3^2 \sim (2\text{–}3)\,u_b^2$: with $U \sim 1$ m s^{-1}, $\epsilon \sim 2\times10^{-5}$ m^2 s^{-3} and $N \sim 2\times10^{-2}$ s^{-1}, this suggests that χ would be overestimated by a maximum of $\sim 1\,\%$. A second estimate is obtained from the magnitude of the largest-scale velocity fluctuations observed in the Class A records: using $\overline{u_1^2} \sim (0.10$ m s$^{-1})^2$, the error is an overestimate of $\sim 3\,\%$.

The degree of error associated with the assumption of isotropy for the dissipation scales of the temperature field is unknown. For the $Pr \gg 1$ case it can be argued that, provided the velocity field achieves isotropy by its dissipation scales, there is no reason to expect anistropy of the temperature field at *its* dissipation scales, since these are even smaller. This argument becomes progressively weaker as the Prandtl number

decreases: indeed Mestayer (1980), working in a laboratory flow at $Pr \simeq 0.7$, provides evidence that the temperature field is anisotropic down to scales as small as $3k_s^{-1}$. Lacking laboratory measurements at $Pr \sim 7$ comparable to those of Mestayer at $Pr \sim 0.7$, there is no choice but to use the isotropic form for χ, even though it is not clear whether $Pr \sim 7$ should be considered 'large' or not.

Before leaving the question of isotropy, it should be noted that the PISCES measurement is of $\overline{(\partial T'/\partial x)^2}$. Thus in extremely anisotropic conditions $\overline{(\partial T'/\partial z)^2} \gg \overline{(\partial T'/\partial x)^2}$ which might be imagined to occur as turbulence decays in a stratified fluid, the true value of χ would be severely *under*estimated by the value calculated from $\chi = 6D\overline{(\partial T'/\partial x)^2}$.

Accuracy of the other parameters used to scale the temperature spectra is also of concern. The turbulent-kinetic-energy-dissipation rate per unit mass ϵ is estimated as

$$\epsilon = 15\nu \int_0^\infty k^2 \phi_{11}(k)\, \mathrm{d}k, \tag{19}$$

using the completely resolved dissipation spectrum of the streamwise velocity component u_1, with $\nu = 1.44 \times 10^{-6}$ m^2 s^{-1} the kinematic viscosity of seawater for the temperature conditions in Knight Inlet. Since the assumption of velocity-dissipation-scale isotropy used in (19) is strongly supported by the observed cross-component spectra (GON), uncertainty in ϵ results only from measurement error and use of the Taylor hypothesis. Measurement error is due mainly to uncertainty in the probe response function at frequencies (wavenumbers) near the peak of the dissipation spectrum. Maximum error of $\sim \pm 6\,\%$ occurs for values of $\epsilon \sim 3 \times 10^{-5}$ m^{-2} s^{-3} characteristic of Class A spectra, when k_s is associated with $f \sim 280$ Hz. For the lowest Class B spectra, where $\epsilon \sim 3 \times 10^{-8}$ m^2 s^{-3} and k_s is associated with $f \sim 50$ Hz, the error is only $\sim \pm 1\,\%$ (Gargett 1980). The effect of Taylor's hypothesis, estimated independently by Lumley (1965) and Heskestad (1965), is to overestimate ϵ by the fraction $(\overline{u_1^2}/u^2) + 2(\overline{u_2^2} + \overline{u_3^2})/(\overline{U})^2$. Using again the two means of estimating velocity-fluctuation variances (see discussion of χ above), the error in ϵ is $\sim 1.5\,\%$ for $\overline{u_1^2} \sim (2\text{–}3)\, u_b^2$ and $\sim 5\,\%$ for $\overline{u_1^2} \sim (0.1 \text{ m s}^{-1})^2$.

Another essential parameter for describing turbulence in a stratified fluid is the buoyancy frequency. Estimates of N were derived from an observed temperature difference ΔT over 0.8 m in the vertical, using the local T/S relation. Error was estimated as 5–11 % over the (high-to-low) observed range of N (GON, §3.3).

5. Results

The range of measured temperature spectra lies between two extremes, associated with either Class A or Class B velocity spectra as defined in §3. Intermediate forms are observed, but it seems sufficient to present these two very clearly different classes. For comparison with theory ψ is non-dimensionalized by

$$\hat{\psi} \equiv \frac{\nu k_s^3}{\chi} \psi = \frac{\epsilon^{\frac{3}{4}}}{\nu^{\frac{5}{4}} \chi} \psi, \tag{20}$$

and plotted as a function of $\hat{k} \equiv k/k_s$, using observed values of ϵ and χ (table 1). Observed spectra are presented in various plots designed to examine three questions: (1) does $\hat{\psi}$ exhibit a $\hat{k}^{-\frac{5}{3}}$ inertial subrange characterized by a universal value of B? (2) does $\hat{\psi}$ exhibit a $\hat{k}^{-1}$ viscous-convective subrange? and (3) is Batchelor's q a

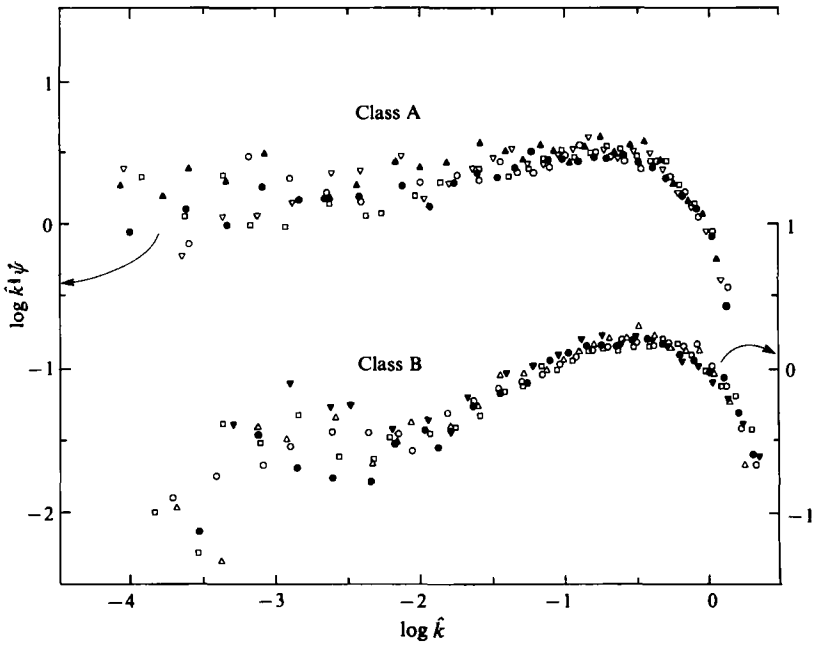

FIGURE 5. Temperature spectra are normalized by the Oboukov–Corrsin scaling $\hat{\psi} = \nu k_s^3 \chi^{-1} \psi$ and plotted here as the $\frac{5}{3}$-*moment spectrum* $\hat{k}^{\frac{5}{3}}\hat{\psi}$ *as a function of normalized wavenumber* $\hat{k} = k/k_s$. The five records from each Class A and B are plotted individually: the symbols associated with each record are shown at the far left of table 1 (these are the same records used to produce the velocity spectra of figure 2). The two classes are here vertically offset by one decade for clarity.

universal constant? Individual records used in each class are plotted as $\frac{5}{3}$ moments in figure 5: since each contains 5 records, for clarity the classes have been shifted vertically by a decade.

5.1. *Inertial subrange?*

The class-averaged $\frac{5}{3}$-moment spectra are plotted in figure 6 within variance error limits for the 5 records in each class. A horizontal region in such a plot indicates an inertial subrange where $\hat{\psi} \sim \hat{k}^{-\frac{5}{3}}$. Variability in the measured spectra is greatest at the lowest wavenumbers, where the error bounds for the two spectra marginally overlap. For wavenumbers $\hat{k} > 10^{-3}$, however, the two classes are totally disjoint (except of course where they cross near $\hat{k} = 1$ because the Class A spectrum rolls off sooner than the Class B spectrum). It is clear that over the range $-4 < \log \hat{k} < -1$ the measured Class A spectrum is not well described by $\hat{k}^{-\frac{5}{3}}$, but by a slightly shallower slope, say $\hat{k}^{-\frac{3}{2}}$. There may be a tendency to approach horizontal, hence $\hat{k}^{-\frac{5}{3}}$ at the lowest wavenumbers, but the spectra do not extend to sufficiently small wavenumbers to show this behaviour conclusively. The Class B spectrum shows a very clear $-\frac{5}{3}$-subrange over approximately the decade $-3 < \log \hat{k} < -2$. Even if one were to argue for approach to a $-\frac{5}{3}$-range at the lowest measured wavenumbers of the Class A spectrum, it is obvious that B is *not* a universal constant. Averages of B over the regions within square brackets on each spectrum in this figure are 1.6 for Class A and 0.35 for Class B.

It seems most unlikely that this variation in B can be explained by errors in calculated values of ϵ or χ. Indeed, since the Class A and B records are quite disjoint at those wavenumbers that might be imagined to make up $\hat{k}^{-\frac{5}{3}}$ subranges, random error cannot be an explanation and we need only examine the magnitudes of the

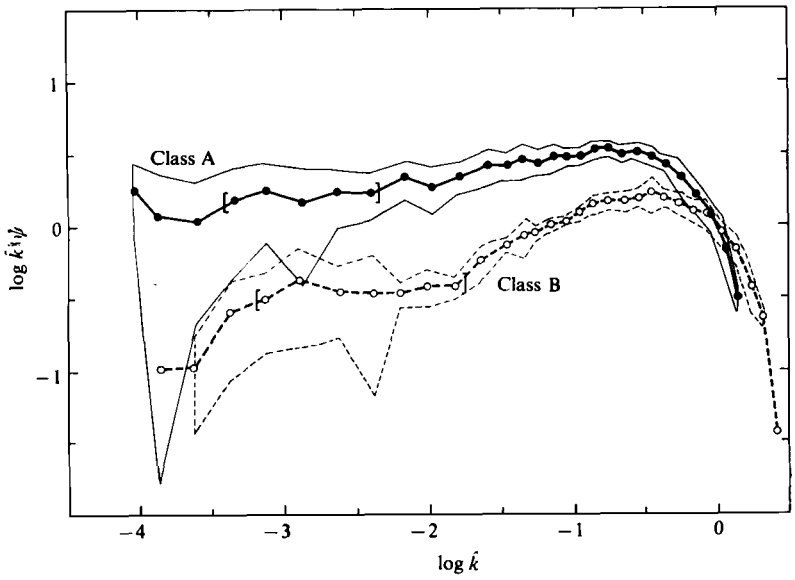

FIGURE 6. Class-averaged values of the $\frac{5}{3}$-moment spectra shown in figure 5, with variance error bars. Note that the Class A spectrum, associated with velocity spectra which fulfil rather stringent conditions for isotropy over the range $-3 < \log \hat{k} < -1$, does not have a clear-cut inertial–convective subrange. An appropriate description would appear to be approximately $\hat{\psi} \sim \hat{k}^{-\frac{5}{3}}$ over the range $-4 < \log \hat{k} < -1$, although some slight flattening in the $\frac{5}{3}$-moment spectrum at the lowest wavenumbers might be an approach to $\hat{k}^{-\frac{1}{3}}$. In contrast, the Class B spectrum has a very distinct $\hat{k}^{-\frac{5}{3}}$ subrange between $-3 < \log \hat{k} < -2$, where the associated velocity spectra do not fulfil isotropic conditions. If one wished to fit $\hat{k}^{-\frac{5}{3}}$ to both spectra (over the limited wavenumber ranges between square brackets, for example), values of the Oboukov–Corrsin 'constant' B would range from 1.6 (Class A) to 0.35 (Class B).

various systematic errors which have been identified. Overestimation of both ϵ and χ by Taylor's hypothesis partially balances in the scaling factor $\epsilon^{\frac{3}{4}}\chi^{-1}$ which occurs in (20); the resulting overestimation of B is only $\sim 1\%$ for the Class A spectra. Anisotropy effects are the other possible candidate for systematic error in ϵ or χ. Since various consequences of isotropy have been directly checked for the dissipation scales of the velocity field, ϵ is unlikely to be substantially in error from this effect. While it is not possible to check the isotropy of the temperature field directly from the submersible measurements, results of laboratory experiments (Lange 1982; Stillinger, Hellend & Van Atta 1983) suggest that the temperature field is most anisotropic during the final stages of decay, a situation surely more similar to the present Class B (in which the velocity field at least is known to have developed anisotropy) than to Class A. As mentioned in the previous section, this implies that χ for Class B might be severely underestimated by our measurement, hence that the non-dimensionalized level of the Class B spectra should be even lower. Clearly neither of these effects eliminates the difference in low-wavenumber levels (hence B values) shown in figure 6.

5.2. *Viscous-convective subrange?*

The class-averaged first-moment spectra are shown in figure 7: a $\hat{k}^{-\frac{5}{3}}$ range appears on this plot as a $\hat{k}^{-\frac{2}{3}}$ range (lines are drawn using the B-values quoted above), while a $\hat{k}^{-1}$ viscous-convective subrange would appear flat. The Class A spectrum clearly

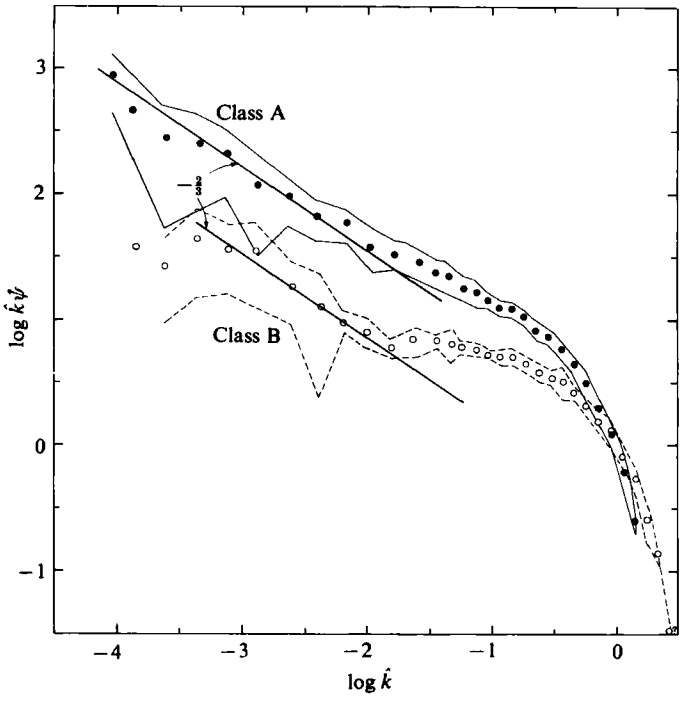

FIGURE 7. The first-moment spectrum $\hat{k}^{+1}\hat{\psi}$ plotted as a function of $\hat{k}$ reveals a viscous-convective subrange $\hat{\psi} \sim \hat{k}^{-1}$ as a flat region. The Class A spectrum clearly has no such region, while the Class B spectrum may be developing one at wavenumbers between $\hat{k} \sim 10^{-2}$ and the diffusive high-wavenumber rolloff. This plot, in which an inertial-convective subrange would appear as a line of slope $-\frac{2}{3}$, again indicates that this is an inappropriate description of the Class A spectrum.

does *not* have a $\hat{k}^{-1}$ subrange. A tendency towards $\hat{k}^{-1}$ develops for non-dimensional wavenumbers above $\hat{k} \sim 10^{-2}$, but even the Class B spectrum cannot be said to exhibit a true $\hat{k}^{-1}$ subrange over any substantial range of $\hat{k}$.

5.3. *Universal diffusive cut-off?*

Variance-preserving plots of dissipation spectra $\hat{k}^2\hat{\psi}$ as a function of $\hat{k}$, shown in figure 8 (*a*), clearly demonstrate that the form of the diffusive cutoff (hence Batchelor's parameter q) cannot be considered universal. To fit the observed spectra by a Batchelor-type function ((15)) in the rolloff region past the peak of the dissipation spectrum, one would need to use $q \simeq 12$ for Class A, but only $q \simeq 4$ for Class B records (figure 8*b*).

One might question this conclusion if it depended entirely upon the observations at the very highest observed wavenumbers, since these are sensitive to the noise-correction procedure used: however, this is not the case. The noise correction is completely negligible for wavenumbers less than $0.3\hat{k}$, and here the observed dissipation spectra are distinctly different. Because the integral under the non-dimensional dissipation spectrum must equal $\frac{1}{6}Pr$, the fact that the observed Class A spectrum lies above the Class B spectrum at low wavenumbers ensures that it must eventually fall below the Class B spectrum at high wavenumbers. In Batchelor's terms, this more rapid high-wavenumber rolloff is characterized by a larger q.

Another effect which can be eliminated as a cause of the observed difference in q is that of fluctuating convection velocity. Fitting the Batchelor high-wavenumber

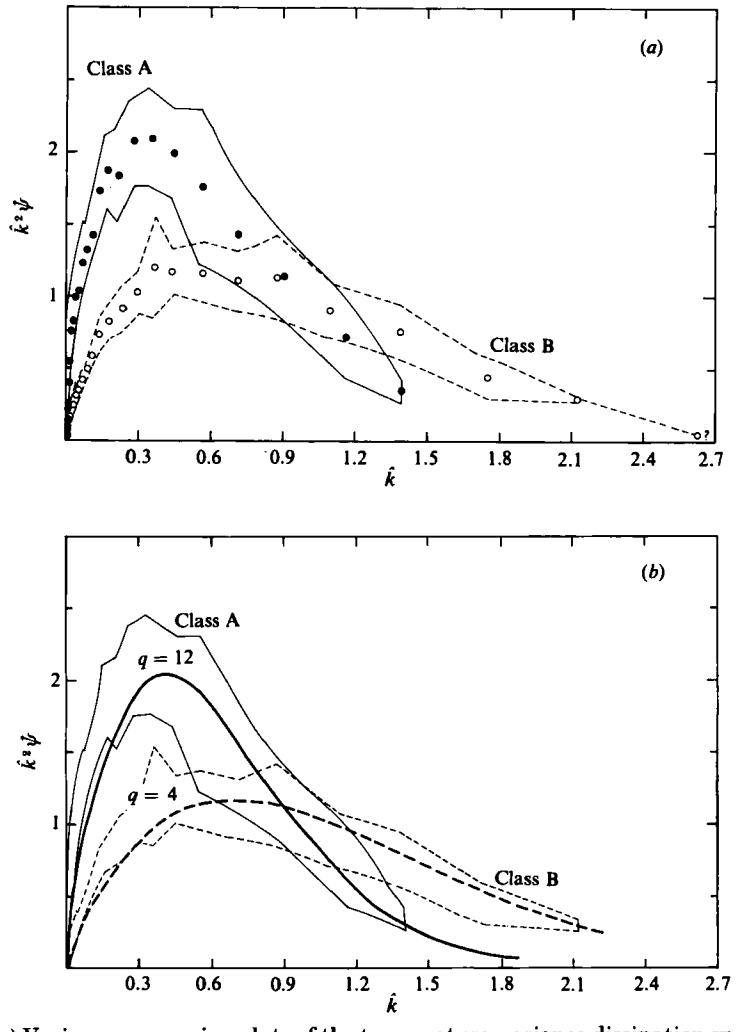

FIGURE 8. (*a*) Variance-preserving plots of the temperature-variance dissipation spectra $\hat{k}^2\hat{\psi}$ for the two classes show that the temperature spectrum is not even universal at the highest wavenumbers of the diffusive rolloff region. (*b*) In terms of the theory of Batchelor (1959), the difference can be expressed as non-universality of the constant q which enters the definition of the least principal rate of strain $\gamma \equiv -q^{-1}(\epsilon/\nu)^{\frac{1}{2}}$ presumed to act on temperature-gradient surfaces. The heavy curves in this figure are curves generated from (15) using values of $q = 12$ (Class A) and $q = 4$ (Class B).

form $\exp(D\gamma^{-1}k^2) = \exp(D\gamma^{-1}\omega^2(U)^{-2})$ using $U = \overline{U}+u$, instead of $\overline{U}$ (where $u_1 \sim 0.1\overline{U}$ at maximum: see §4), could change the effective γ, hence q, by $\pm 20\%$, but this is far short of the actual observed differences.

6. Discussion

Previous observations of the spectrum of temperature in water ($Pr \sim 7$) have produced a composite of the features expected of the spectrum of a passive scalar at high Reynolds and Prandtl numbers. These features, with some of the studies taken as confirmation, are:

(i) a $k^{-\frac{5}{3}}$ inertial-convective subrange with the 'universal constant' $B \sim 0.55$ a weak function of Re_λ (Gibson & Schwartz 1963, hereinafter GS; Grant *et al.* 1968,

hereinafter GHVM; Boston & Burling 1972, hereinafter BB; Champagne *et al.* 1977, hereinafter CFLW; Williams & Paulson 1977, hereinafter WP), followed at higher wavenumbers by

(ii) a rise to a k^{-1} viscous-convective subrange (GS, GHVM), then finally by

(iii) a diffusive rolloff region characterized by a value $q \sim 4$ in the shape (15) proposed by Batchelor (Dillon & Caldwell 1980; Oakey 1982).

For brevity, I will call this composite the Batchelor spectrum, although of course the inertial-convective subrange pre-dates Batchelor (1959).

The present observations combine two features not achieved simultaneously by previous measurements: determination of ϵ and χ by direct integration of the respective dissipation spectra; and the ability to check requirements of velocity-field isotropy, such as (4) and (5), which are more stringent than the mere existence of a $k^{-\frac{5}{3}}$ subrange in the streamwise-velocity-component spectrum. The results of these observations are surprising to say the least. The Class A records have the highest values of Re, have energy-containing scales on average three thousand times larger than the length $l_s \equiv 2\pi/k_s$ associated with the Kolmogoroff wavenumber, and fulfil condition (4) for velocity-field isotropy over almost the entire measured range of wavenumbers: however, the associated temperature spectra have *none* of the characteristics usually attributed to the Batchelor spectrum. Instead of distinct subranges with slopes of $-\frac{5}{3}$ and -1, the Class A temperature spectra have a subrange of intermediate slope ($\sim -\frac{3}{2}$) which extends to a dissipative roll-off range which is characterized by a value $q \sim 12$ if Batchelor's form (15) is fitted at the highest wavenumbers. Even more curiously, *all* of the elements of the Batchelor spectrum appear to develop as the field evolves to Class B, cases where the velocity field has certainly developed measurable anisotropy at wavenumbers within the pseudo-'inertial-convective' subrange of the scalar spectrum. Moreover, the vertical energy-containing wavenumber k_b is constrained by buoyancy to a range of $k_s/(50\text{–}100)$: since the velocity-dissipation spectrum begins to rise steeply past $k_s/100$, it is clear that there can be no large separation between energy-input and dissipation scales as required for the notion of a three-dimensional turbulent energy cascade.

These results suggest the following conclusions. First, there is no universal inertial-convective subrange: in the present observations, the high-Reynolds-number shape of the passive-scalar spectrum appears to be approximately $k^{-\frac{3}{2}}$ rather than $k^{-\frac{5}{3}}$. Secondly, a pseudo-$k^{-\frac{5}{3}}$ subrange appears and persists (while moving to lower non-dimensional level, hence lower 'B'-value) as the smallest dimension of the energy-containing eddies (here the vertical dimension) approaches a scale $\sim l_s/100$ typical of the low-wavenumber end of the velocity-dissipation spectrum. Thirdly, during this evolution of the $k^{-\frac{5}{3}}$ subrange, the slope of the temperature spectrum above approximately $\hat{k} \simeq 0.01$ (but below the abrupt viscous-diffusive rolloff) evolves from approximately $k^{-\frac{3}{2}}$ towards k^{-1}. Finally, the high-wavenumber rolloff of the temperature spectrum is no more universal than the low-wavenumber end.

Since these conclusions are startling in view of the widespread acceptance of the Batchelor spectrum as an appropriate fit to the spectrum of temperature fluctuations in water, it seems necessary to review the previous observational basis of that acceptance in view of the framework provided by the present observations. It must be immediately clear from the results shown in §5 that an acceptable determination of the various slopes, shapes and levels involved in the Batchelor spectrum must *at an absolute minimum* determine both ϵ and χ simultaneously and directly, rather than by adjusting measured low-wavenumber spectral levels to fit 'universal' curves (a procedure which of course assumes rather than tests the universal nature of the

curves). This requirement eliminates one of the classical references in the field, since GHVM were unable to determine χ directly because of electronic noise in their cold-film circuit, hence used the fit of the Batchelor spectrum at low wavenumber to determine χ. Without independent knowledge of χ, this procedure forces B (their β_1) to be approximately constant: their determinations range from 0.13 to 0.47, a difference of a factor of ~ 4. Given the framework of the present observations, forcing B to be approximately constant should result in considerably more variation in other fitted parameters of the Batchelor spectrum. Indeed, GHVM fitted values of k_*/k_s, where k_* is the wavenumber of the intersection of $k^{-\frac{5}{3}}$ and k^{-1} subranges, and found values varying by a factor of ~ 7, while fitted values of q varied by a factor of ~ 18. Although the Discovery-Passage measurements have long been considered a case of high Reynolds number (based upon tidal velocity and depth of the channel, $Re \sim 3 \times 10^8$), most of the reported temperature spectra were taken outside Discovery Passage itself. Given the temperature and salinity stratification reported for the region outside the Passage (their figure 2), indicating a salinity change of $\sim 6‰$ and a temperature change of ~ 6 °C over the top 25 m within which all the reported runs were made, it seems possible that mean stratification sufficient to restrict vertical scales was present even after a full ebb/flood cycle in the area. In the additional offshore measurements presented, GHVM point out characteristics of the observed velocity spectra which suggest low Reynolds number. If all the measurements of GHVM were characterized by vertical scale limitation, then their observations of $-\frac{5}{3}$ and approximate -1 subranges would be consistent with the present Class B spectra.

The other set of observations frequently used to demonstrate $k^{-\frac{5}{3}}$ and k^{-1} scalar subranges, and to determine values for B and q, is the laboratory grid-turbulence data of GS. Here, dissipation rates ϵ and χ (or χ_s, the salinity-fluctuation dissipation rate, depending upon whether T or S was used as a stratifying property) were determined indirectly by differentiating observed linear-decay laws for velocity or scalar variance with distance from the grid. These rates satisfactorily collapsed the streamwise velocity spectrum $\phi_{11}(k)$ to a universal high-wavenumber shape, with an apparent inertial subrange which increased in length towards low wavenumbers with increase in grid Reynolds number: the maximum observed extent of this subrange was approximately one decade, equivalent to the present Class B (figure 2). The addition of χ (or χ_s) collapsed the observed scalar spectra to 'universal' forms: however, in this case it seems quite probable that the observed $k^{-\frac{5}{3}}$ and approximation of k^{-1} subranges observed in those parts of the scalar spectra which were resolved, both result from vertical scale limitation. Using the height $h = 6$ inches (~ 15 cm) of the laboratory test section to form a minimum possible vertical wavenumber $k_m = 2\pi/h$, the estimated isotropy ratio $I \equiv k_s/k_m$ ranges from ~ 400 for the maximum value of $k_s = 170$ cm^{-1} reported in figure 3 of GS, to ~ 45 for the minimum value of $k_s = 19$ cm^{-1}, a range in rough agreement with the I-values which characterize the Class B spectra of this paper. The observed 'inertial' subrange in the streamwise velocity spectrum is, of course, not inconsistent with the conclusion that these measurements are actually characteristic of vertical scale-limited turbulence, rather than high-Reynolds-number homogeneous isotropic turbulence.

The more recent oceanographic literature generally fails to achieve the requirement of simultaneous and direct determination of ϵ and χ. Dillon & Caldwell (1980) did not determine ϵ directly, while Gregg & Sanford (1980) were forced to use an ϵ-value determined directly but not at the same place or time as their χ determination. The exception is the work of Oakey (1982), who calculated both ϵ and χ directly from measurements made by a single instrument, hence scaled observed temperature

spectra without ambiguity. Although problems of sample inhomogeneity (in vertical profiles from the upper stratified ocean) produced rather scattered results, Oakey calculated an overall average value of $q \sim 3.7$, very close to the value associated with the present Class B spectra. At wavenumbers below the dissipative rolloff his dissipation spectra $k^2\psi$ and those of Dillon & Caldwell (1980) both exhibit slopes between a value of $\sim +\frac{1}{2}$, which would correspond to the approximate $-\frac{3}{2}$ slope of the Class A temperature spectra, and a value of $+1$, which would suggest that a temperature spectral slope of -1 is a limiting value for buoyancy-affected temperature spectra. Note, however, that this behaviour is just the opposite to that expected (Dillon & Caldwell 1980) if it is assumed that $\psi \sim k^{-1}$ represents the temperature spectrum of the most active (isotropic) cases.

Before leaving the subject of past evidence for the existence of a viscous-convective subrange, it is worth while to emphasize that the physical model underlying Batchelor's derivation of $\psi \propto k^{-1}$ (§1) absolutely requires that any such subrange should occur for $k > k_s$, not the range $k < k_s$ where such a spectral shape has been observed.

Since a true inertial-convective subrange should be independent of Pr, additional information for this region can be obtained from the atmospheric-boundary-layer measurements mentioned in §1 (WP, CFLW, BB). It appears possible that these measurements, like the oceanic ones, are affected by a limit on the vertical scale of turbulent eddies, hence on the 'room' in wavenumber space for development of a true inertial subrange with all its consequences. For unstable and neutrally *stable* atmospheric boundary layers, an appropriate definition of an isotropy ratio would be

$$I_{BL} \equiv \frac{l_0}{l_s},$$

where l_0 is a vertical turbulent lengthscale which is constrained, through the mean-shear structure, by the presence of a solid boundary. From reported values of ϵ, associated values of $l_s \equiv 2\pi/k_s$ range from a minimum of ~ 0.25 cm (WP) to ~ 0.66 cm (BB). Using the height z of the measurement as the maximum possible vertical eddy size, maximum possible isotropy ratios range from ~ 400 (WP, who made measurements at 2 m height) to ~ 950 (BB and CFLW, both with instruments at 4 m): if the actual vertical lengthscale is some fraction of z, these values would of course be less. Although not presented here, records with isotropy ratios in this range, between those characteristic of Class A and those characteristic of Class B, exhibit intermediate characteristics; namely a decrease in (non-dimensionalized) low-wavenumber level (the parameter B), and the appearance of a high-wavenumber 'bump', as the k^{-1} range evolves. Both WP and CFLW observed a similar 'bump', a slight flattening of the $k^{-\frac{5}{3}}$ inertial-convective subrange just before the diffusive high-wavenumber rolloff of the temperature spectrum. This 'bump' has been the source of some speculation (Williams & Paulson 1977; Hill 1978; Herring *et al.* 1982) since Batchelor's theory was not expected to apply to a low-Prandtl-number fluid like air. In the present view, given the isotropy ratios estimated above, the 'bump' is probably associated with a 'low' isotropy ratio. Unfortunately, neither WP nor CFLW reported vertical velocity spectral shapes, so they cannot be checked for the existence of a similar 'bump'. However, measurements of the three-dimensional velocity field in the lower atmospheric boundary layer typically find vertical velocity variance $\overline{u_3^2} < \overline{u_1^2}$ even in unstable conditions (CFLW report $\overline{u_3^2} \sim (\frac{1}{2}-\frac{1}{3})\overline{u_1^2}$; see also Kaimal *et al.* 1972; Weiler & Burling 1967). Thus, by continuity alone, a typical

	ρ	m	B'
Class A	0	-1.55	$1.25B$
Class B	$+0.67$	$-1.67\ (-\frac{5}{3})$	B
	$\mu = \mu_\theta = 0.5$	$A = A_\theta = 1$	

TABLE 2. Using observed correlation coefficients ρ between $\ln \epsilon$ and $\ln \chi$ for the two classes and the theory of Van Atta (1971, 1973) (with additional parameter values $(\mu, \mu_\theta, A, A_\theta)$ noted below), modified values are predicted for the slope m and 'universal' scaling parameter B' associated with an inertial–convective scalar spectral subrange.

vertical scale l_0 must be less than a typical horizontal scale l_H for the boundary-layer measurements. Existence of this large-scale anisotropy suggests that the associated temperature spectra should to some degree exhibit characteristics similar to those of the Class B spectra. A temperature spectrum more similar to the Class A spectra has been reported by BB. The low-wavenumber end of their spectrum is associated with a much larger value of $B = 0.8$ than any reported by WP or CFLW, while the high-wavenumber end exhibits no 'bump'. Although both characteristics suggest a larger isotropy ratio, values estimated using $l_0 \sim z$ and values of ϵ reported by BB do not greatly exceed those of the other two studies. The difference may be real, associated in some way with differences of actual vertical scales in boundary layers over a smooth mud flat (BB) or over ploughed (CFLW) or grassy (WP) fields, or it may be an artefact associated with the humidity sensitivity of cold wires in a marine environment (Schmitt, Friehe & Gibson 1978).

From the above discussion, it is apparent that future finescale measurements in the atmospheric boundary layer should include vertical velocity measurements through dissipation scales, as well as observations over the largest possible range of Re, if rationalization of atmospheric and present measurements is to be tested.

Having found that much previous observational evidence for the Batchelor spectrum is either inadmissible or in rough agreement with various features of the present observations, it is still necessary to consider whether the difference between Classes A and B might be caused by differences between the two classes in the degree of intermittency in ϵ and χ. To assess the effects of intermittency, I have used the theoretical framework of Van Atta (1971, 1973) for the inertial-convective subrange, as discussed in §1. Streamwise-velocity and temperature records were divided into pieces of approximate length $l_s/100$ and ϵ and χ were calculated by integration of the respective noise-corrected dissipation spectra. The correlation coefficient ρ between $\ln \epsilon$ and $\ln \chi$, calculated for each class separately, is given in table 2, along with derived values of the inertial-convective subrange slope m and the constant B' calculated with $\mu = \mu_\theta = 0.5$ and $A = A_\theta = 1$. It is interesting to note that $\rho \sim \frac{2}{3}$ for the Class B spectra, a value which results in exactly the classical $-\frac{5}{3}$ slope. The value of $\rho \sim 0$ for the Class A spectra produces the correct qualitative effects of decreasing the spectral slope and increasing the inertial-convective range constant: however the latter effect falls short of the observed ratio (about 4) between the low-wavenumber levels of the two classes. Although there is no complete theory for the effect of intermittency on the dissipative ranges of the temperature spectrum it is interesting to note that the calculated values of the correlation coefficients also have consequences at these much higher wavenumbers. A value of $\rho \sim 0$ implies no correlation between regions of high ϵ and regions of large χ. This in turn implies that regions of

high χ can be considered to be acted upon by the most probable rate of strain, i.e. by the mode rather than the mean of the rate-of-strain distribution. Since the mode γ_0 is smaller than the mean γ_m for a skewed distribution such as that of ϵ, this suggests that, for Class A records, the effective rate of strain $(\gamma)_A \sim \gamma_0 \ll \gamma_m$; thus finally

$$|(\gamma)_A| \equiv \frac{1}{q_A}\overline{\left(\frac{\epsilon}{\nu}\right)^{\frac{1}{2}}} \ll \overline{\left(\frac{\epsilon}{\nu}\right)^{\frac{1}{2}}} = \gamma_m$$

must have $q_A \gg 1$. As ρ approaches the value of $+\frac{2}{3}$ characteristic of the Class B records, larger values of χ have become associated with larger values of ϵ; hence the effective rate of strain $(\gamma)_B$ has become closer to the mean: qualitatively then, $q_B < q_A$, in agreement with observation.

Although the qualitative features of the intermittency effects are certainly in the right directions, there are problems with the underlying assumptions of the present theory. In particular, the assumption that the outer turbulent lengthscale L is much larger than the scale (here $r = l_s/100$) over which ϵ and χ are calculated, is clearly not satisfied for the Class B spectra: also the distribution functions of ϵ and χ do not appear to be particularly well described as lognormal in this case. A more complete study of the ϵ and χ statistics is at present underway, with the aims of improving the description of these statistics and discovering whether the observed range of B-values is indeed outside a range which could be caused by intermittency.

Finally, I would like to return to the question of the evolution of a k^{-1} subrange in the temperature spectrum. This subrange occurs under conditions which cannot be those required by Batchelor (1959), where the least principal turbulent rate of strain $\gamma \propto (\epsilon/\nu)^{\frac{1}{2}}$ is constant over dimensions within which temperature variance is destroyed by molecular effects. However, the derivation of the k^{-1} form can be considered as merely a dimensional argument employing *some* rate of strain; hence an obvious question is whether there is some other strain rate which *can* be considered to be constant over such dimensions and which may be used in place of γ in (15). Since energy exchange between overturning motions and internal waves is a characteristic of a stratified fluid, an obvious choice is N, the internal-wave rate of strain. Thus we ask if it is possible to collapse the observed k^{-1} range (or approximation thereto) in the Class B spectra to a 'universal-internal-wave-strained' form by scaling $\psi(k)$ by χN^{-1} and frequency by N. This scaling, shown in figure 9, is unsuccessful, a result which is actually contained in the obvious success (figure 3) of the Kolmogoroff scaling (20) over the considerable range of $I = [(\epsilon/\nu)/N^2]^{\frac{3}{4}}$ found within Class B. The success of the choice $\gamma \propto (\epsilon/\nu)^{\frac{1}{2}}$ rather than N suggests that it is not just the ratio of turbulent to internal-wave rate of strain which determines the evolution of the temperature spectral shape (otherwise all records in Class B would have the same I-values), and that some type of strongly nonlinear process is still dominant.

An alternative explanation for the observed appearance of a k^{-1} subrange can be based upon a model of the 'large' eddies of the turbulent field. Previous evidence (§3) suggests that the largest eddy which can just overturn in a mean gradient $\partial T/\partial z \propto N^2$ has vertical scale $l_0 \sim k_b^{-1}$ and velocity variance $u^2 \propto u_b^2$. Let us assume that eddies of this size lose a large fraction of their energy and associated temperature variance by cascade to smaller scales within one eddy overturning time τ. This is an established result for homogeneous turbulence (Batchelor & Townsend 1948; see also Batchelor 1959, §6.1) and would seem to have even more justification for stratified turbulence, since if an eddy of size l_0 has just enough energy to overturn, by the time it has lost energy to smaller scales, it can no longer overturn at that scale. The

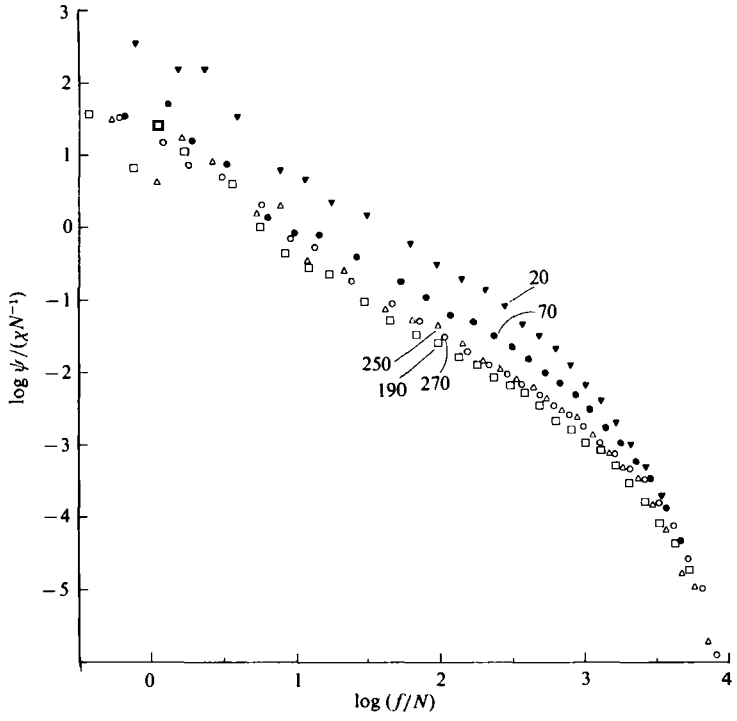

FIGURE 9. Class B records are here non-dimensionalized using an internal-wave rate of strain $\propto N$ in place of the turbulent rate of strain $\propto (\epsilon/\nu)^{\frac{1}{2}}$: for consistency, frequency is non-dimensionalized by N. Values of the isotropy ratio $I \equiv k_s/k_b$ are noted for each record. This was an attempt to discover another relevant constant rate of strain which, when used in Batchelor's (1959) arguments, would predict a k^{-1} behaviour of the temperature spectrum. This scaling is clearly unsuccessful, failing to collapse the k^{-1} ranges (or approximations thereof) of the Class B spectra to a universal curve.

kinetic-energy balance (Tennekes & Lumley 1972) yields the scale relation

$$\frac{u^2}{\tau} \sim \epsilon, \tag{21}$$

which with $\tau \propto N^{-1}$ implies $u^2 \sim \epsilon/N \simeq u_b^2$, consistent with observations. Note that (21) is valid provided that the ratio of potential- to kinetic-energy dissipation rate is small and/or constant. The last column of table 1 is an attempt to estimate this ratio: the average value of 0.28 seems sufficiently small (and constant) to validate (21). A simplified balance of temperature variance for scales smaller than l_0 is:

$$\frac{\partial(\frac{1}{2}\overline{(T')^2})}{\partial t} = \overline{u_3 T'}\,\frac{\partial T}{\partial z}, \tag{22}$$

with the understanding that the variance delivered to the cascade is eventually delivered to dissipation scales. Taking θ and w as the magnitudes of typical temperature and vertical velocity fluctuations respectively, this equation scales as

$$\frac{\theta^2}{\tau} \sim w\theta N^2.$$

Using $\tau \sim N^{-1}$,

$$\theta \sim wN,$$

apart from some dimensional constants. This relation suggests that the temperature fluctuations may be derived from the vertical velocity fluctuations. The approach to a k^{-1} range in the temperature spectrum may thus simply reflect the approach to a k^{-1} range which is observed in the vertical velocity spectrum (figure 1).

This 'theory' has an implicit inconsistency however, for (22) could also be written as

$$\frac{\partial(\frac{1}{2}\overline{(T')^2})}{\partial t} = \chi; \tag{23}$$

hence

$$\theta^2 \sim \chi N^{-1},$$

exactly the internal-wave scaling which was just found to be unsuccessful (figure 9). I will shortly suggest that the balance (23) may not be correct as written, because the measured scalar-dissipation rate χ may be supplied only partly by the scales which supply energy to smaller scales at rate ϵ.

The above explanation also has the obvious disadvantage of merely moving the question, since we now must ask why the vertical velocity spectrum has a k^{-1} range under vertical scale-limited conditions. Nevertheless, it may serve the purpose of emphasizing that the k^{-1} subranges that have been observed in the spectra of temperature fluctuations in water may (and probably do) arise for reasons quite different from those of Batchelor (1959). It is likely that a true viscous-convective subrange has not yet been observed (although with sufficient instrument resolution there is no reason to suppose that it might not be observed in cases of much higher Pr, where there is substantial separation between k_s and k_B).

Another feature which invites speculation is the appearance of a short but distinct $k^{-\frac{5}{3}}$ subrange in the scale-limited conditions of Class B. It seems quite probable that this arises as the spectrum of passive scalar fluctuations advected by nearly horizontal wave motions. The question of what is wave and what is turbulent motion is of course an extremely difficult one (Stewart 1969). I am going to use a definition which is rather simple to state and to use conceptually, namely that turbulent motions transfer energy irreversibly and efficiently to ever smaller scales while wave motions do not. Observationally, this definition cannot be tested: I simply assume that the division in character occurs in wavenumber space near the wavenumber k_b associated with the largest possibly-isotropic scale. These largest isotropic eddies (scale $l_0 \sim k_b^{-1}$) can lose energy by one of two means, either by supporting an energy cascade to smaller scales or by generating internal waves: in fact they probably do both in some unknown combination. In the model of the k^{-1} subrange presented above, it was assumed that most of the energy was transferred to turbulent motion at higher wavenumbers. Consider now the effect of using some part of that energy to force wave motions.

For linear waves in a fluid of (locally) constant N, the magnitude of the wave vertical velocity w_i is given by

$$|w_i| = \frac{\alpha n}{N}$$

where n is wave frequency and $\alpha = (u_i^2 + v_i^2 + w_i^2)^{\frac{1}{2}}$ is the root-mean-square wave velocity (Philips 1977). Rearranging this relation, the frequency can be expressed as

$$n = N\left[\frac{w_i^2}{u_i^2 + v_i^2 + w_i^2}\right]^{\frac{1}{2}} = N\left[\frac{1}{1+2a^2}\right],$$

where the anisotropy ratio $a \equiv |u_i/w_i| = |v_i/w_i|$ has been introduced. When the forcing velocity field is isotropic (Class A), $a = 1$ and $n = N/\sqrt{3}$. Since $n = N\cos\beta$, β being the angle between wavenumber vector $\boldsymbol{k}$ and vertical, this corresponds to a propagation direction of $\sim 55°$ from vertical. As the velocity field becomes influenced by buoyancy (Class B), a increases and n decreases; hence the wavenumber vector $\boldsymbol{k}$ approaches vertical. Thus as the anisotropy of the forcing field (the largest overturning eddies) increases, the forced internal-wave field approaches the limit of horizontal plane motion.

Although this forced-field analysis has been in terms of linear waves, it seems likely that, as amplitudes grow under continued forcing, nonlinear wave transfer will become important. Thus it may not be unreasonable to consider results from two-dimensional 'turbulence', which predict $k^{-\frac{5}{3}}$ slopes of the (horizontal) energy spectrum (perhaps explaining the persistence and extent of the $k^{-\frac{5}{3}}$ subrange in the horizontal-component spectrum ϕ_{11}) *and* of the associated passive-scalar spectrum (Lesieur & Herring 1985). Lesieur & Herring, as well as Holloway & Kristmannsson (1984), also show that, while energy is transferred to lower wavenumbers as well as to higher wavenumbers, the *scalar* variance transfer is to ever smaller scales. Thus in such systems the scalar variance dissipated at rate χ at small scales does not all originate from the same scales (near k_b^{-1}) which support the *energy* flux to small scales. Such a characteristic would remove the inconsistency mentioned above in discussion of the k^{-1} subrange, and help to explain why temperature spectra are considerably less universal in character, even at the smallest scales, than associated velocity spectra.

7. Conclusions

The present observational evidence suggests that the Corrsin–Oboukov–Batchelor description cannot be used as a universal description of the spectrum of temperature fluctuations in water. Reasons underlying the discrepancies between theories and observations may be different in the two classes presented. The more isotropic Class A spectra may differ because of intermittency effects, while the Class B spectra may be characteristic of a non-passive scalar spectrum (since the limitation of vertical scale, the basis of all the explanations proferred in §6 for at least the sense of the Class B characteristics, arises through the stable stratification: while the temperature itself does not determine the density in Knight Inlet, it is everywhere linearly related to salinity, which does). Appropriate theory for the latter case is clearly a major theoretical challenge, involving as it does the subtleties of wave/turbulent dynamics and the directional anisotropies of the system.

The measurements were accomplished through the technical skills of G. Chase, R. Teichrob and L. Beauchemin, exercised over years of (often unsuccessful) fieldwork: I thank them also for their perseverance. The contributions of the pilots of PISCES IV and the officers and crew of the PANDORA II are gratefully acknowledged.

Appendix. The cold-film measurement

High-frequency temperature fluctuations were measured with an unheated conical platinum-film sensor (Thermo-Systems Model 1230T) on which the film covers the cone tip. The sensor (resistance 5–10 Ω) is used as one leg of an a.c. bridge driven by an amplitude-stable 11.2 kHz oscillator. The actual bridge, driver and detector

were placed in an underwater pressure case immediately behind the probe in order to minimize lead resistance, which may otherwise prove significant relative to the small probe resistance. Remaining circuitry was located within the manned sphere of the submersible. Approximately 50 mV r.m.s. voltage is applied across the probe, and a balancing resistor is adjusted to give an approximate bridge balance at the mean water temperature T_W. The bridge can then be pseudo-balanced at any temperature within a range $\pm T_R$ about T_W by summing the amplified bridge signal with a reference consisting of the oscillator voltage adjusted manually in both phase and amplitude. Output of the summing amplifier appears to be that of a balanced bridge, as any change in temperature of the probe produces deviations from the null point of the summing amplifier. Final output from the bridge is a d.c. voltage with a variable gain of $G = 1$, 2 or 4 times A_0, the zero-frequency gain of the probe/bridge system. The frequency response of this system is $A(f)\,L(f)$, where $A(f)$ is the response characteristic of the probe itself and $L(f)$ is the response of a low-pass filter (3 db at 300 Hz) included to minimize aliasing upon digitization at a sample rate of 1000 Hz. Further filtering includes a high-pass filter (3 db at 0.5 Hz) and a gain of 11 in the pass band) to limit the dynamic range of the high-frequency temperature channel, and a pre-whitening filter with zero-frequency gain of 2 and a response $W(f)$ designed to maintain the low-frequency signal-to-noise ratio to the highest measured frequencies despite probe rolloff. Raw power spectral densities for temperature $\psi_r(f)$ [volts^2/Hz] are thus converted to physical units and response-corrected by:

$$\psi_T(f)\,[(^\circ\mathrm{C})^2/\mathrm{Hz}] = \frac{\psi_r(f)\,[\mathrm{volts}^2/\mathrm{Hz}]}{(S_0\,S(f))^2}$$

where

$$S_0 = A_0\,G \times 11 \times 2$$

and

$$S(f) = A(f)\,L(f)\,W(f), \quad S(f=0) = 1.$$

The normalized filter response functions $L(f)$ and $W(f)$ are measured directly, while the probe/bridge characteristics A_0 and $A(f)$ are determined experimentally, as described in the following paragraph. No correction is made for the high-pass filter rolloff since this is negligible for the frequencies $f \gtrsim 1$ Hz at which the cold-film signal is used.

A_0 was measured with the probe soldered into its final configuration on PISCES, because probe resistance is sufficiently small that changes in lead resistance before the bridge affect this calibration. The probe was immersed in vigorously stirred water in an insulated flask and calibrated against a Hewlett–Packard quartz thermometer over about a 10 °C range. Even on the lowest gain setting, the temperature circuit traverses full scale (± 10 V) over ~ 3 °C; the bridge was re-balanced each time full scale was reached; hence a typical calibration consisted of two or three separate sections. A_0 is the slope of this linear calibration, obtained by averaging the slopes obtained by least-squares linear fits to each individual section. The field calibration in Knight Inlet (22 November) yielded a value of $A_0 = 0.4084$ volts/°C $\pm 0.14\,\%$. A continual check on the low-frequency gain of the platinum thermometer is provided by simultaneous measurements from the nearby thermistor (see below). Within their range of overlap, spectral levels from the two thermometers always agree within their respective statistical uncertainties.

The frequency response $A(f)$ was determined by the plume-tank method originated by Fabula (1968), as subsequently refined by Hughes (see appendix to Fabula 1968). A thermistor is tracked slowly ($U_{th} = 0.02$ cm s^{-1}) through the steady narrow

convective plume rising from a single heated wire stretched across a calibration tank. The thermistor is then removed and the cold-film probe is shot across the plume at a constant speed U_p. The ratio of the power-spectral density of the platinum thermometer signal to that of the thermistor signal (scaled in frequency to allow for the different speeds at which the two probes traverse the constant domain in physical space) then yields $A(f)\,A^*(f)$, the square of the magnitude of the (complex) platinum response function $A(f)$. According to the theory of Fabula, $|A(f)| = \exp(-(\Delta^2\pi f/D)^{\frac{1}{2}})$ where f is frequency in Hz, D is the thermal diffusivity of water, and Δ is a lengthscale of the order of the velocity boundary-layer thickness over the film. A plot of $\ln|A(f)|$ against $f^{\frac{1}{2}}$ yields a straight line through (0, 0) with slope $-[\Delta^2\pi/D]^{\frac{1}{2}}$, from which the parameter Δ may be determined. At a calibration speed $U_p = 1$ m s^{-1} comparable to the mean operating speed of PISCES, this technique yielded $\Delta = 2.17 \times 10^{-3}$ cm $\pm 1.3\%$ for the probe used in the present measurements. For each record this value is adjusted for slight differences in mean speed, kinematic viscosity and thermal diffusivity between calibration (laboratory) and field conditions, using the Reynolds-number and Prandtl-number scalings suggested by Fabula and Hughes (Fabula 1968).

Because the measured parameter Δ occurs in an exponential function, the associated error in ψ_T increases with frequency, from 0 % at $f = 0$ Hz to approximately ± 1 % at $f = 10$ Hz, ± 3 % at $f = 100$ Hz, and ± 6 % at the Nyquist frequency of $f = 500$ Hz. Thus error in ψ_T is due mostly to error in A_0 at low frequencies, but becomes dominated by error in Δ at the higher frequencies (wavenumbers) which dominate dissipation spectra for temperature variance, hence estimates of χ.

REFERENCES

Antonia, R. A. & Van Atta, C. W. 1975 On the correlation between temperature and velocity dissipation fields in a heated turbulent jet. *J. Fluid Mech.* **67**, 273–288.

Batchelor, G. K. 1959 Small-scale variation of convected quantities like temperature in turbulent fluid. *J. Fluid Mech.* **5**, 113–133.

Batchelor, G. K. & Townsend, A. A. 1948 Decay of isotropic turbulence in the initial period. *Proc. R. Soc. Lond.* A **193**, 539–558.

Boston, N. E. J. & Burling, R. W. 1972 An investigation of high-wavenumber temperature and velocity spectra in air. *J. Fluid Mech.* **55**, 473–492.

Champagne, F. H., Friehe, C. A., LaRue, J. C. & Wyngaard, J. C. 1977 Flux measurements, flux estimation techniques and fine-scale turbulence measurements in the unstable surface layer over land. *J. Atmos. Sci.* **34**, 515–530.

Corrsin, S. 1951 On the spectrum of isotropic temperature fluctuations in isotropic turbulence. *J. Appl. Phys.* **22**, 469–473.

Crawford, W. R. 1985 A comparison of lengthscales and decay times of turbulence in stably stratified flows. *J. Fluid Mech.* (submitted)

Dillon, T. M. 1982 Vertical overturns: a comparison of Thorpe and Ozmidov length scales. *J. Geophys. Res.* **87**, 9601–9613.

Dillon, T. M. & Caldwell, D. R. 1980 The Batchelor spectrum and dissipation in the upper ocean. *J. Geophys. Res.* **85**, 1910–1916.

Dougherty, J. P. 1961 The anisotropy of turbulence at the meteor level. *J. Atmos. Terr. Phys.* **21**, 210–213.

Farmer, D. M. & Smith, J. D. 1980 Tidal interaction of stratified flow with a sill in Knight Inlet. *Deep-Sea Res.* **27A**, 239–254.

Gargett, A. E. 1980 Data Report and calibrations of turbulence measurements in Knight Inlet, B.C. from the PISCES IV submersible: November 1978. *Pacific Marine Sci. Rep.* 80-6. Institute of Ocean Sciences, Patricia Bay, P.O. Box 6000, Sidney, B.C., Canada. 71 pp.

GARGETT, A. E., HENDRICKS, P. J., SANFORD, T. B., OSBORN, T. R. & WILLIAMS, A. J. 1981 A composite spectrum of vertical shear in the upper ocean. *J. Phys. Oceanogr.* **11**, 1258–1271.

GARGETT, A. E., OSBORN, T. R. & NASMYTH, P. W. 1984 Local isotropy and the decay of turbulence in a stratified fluid. *J. Fluid Mech.* **144**, 231–280.

GIBSON, C. H. & SCHWARZ, W. H. 1963 The universal equilibrium spectra of turbulent velocity and scalar fields. *J. Fluid Mech.* **16**, 365–384.

GIBSON, C. H., STEGEN, G. R. & MCCONNELL, S. 1970 Measurements of the universal constant in Kolmogoroff's Third Hypothesis for high Reynolds number turbulence. *Phys. Fluids* **13**, 2448–2451.

GIBSON, C. H., STEGEN, G. R. & WILLIAMS, R. B. 1970 Statistics of the fine structure of turbulent velocity and temperature fields measured at high Reynolds number. *J. Fluid Mech.* **41**, 153–167.

GRANT, H. L., HUGHES, B. A., VOGEL, W. M. & MOILLIET, A. 1968 The spectrum of temperature fluctuations in turbulent flow. *J. Fluid Mech.* **34**, 423–442.

GRANT, H. L., STEWART, R. W. & MOILLIET, A. 1962 Turbulence spectra from a tidal channel. *J. Fluid Mech.* **12**, 241–263.

GREGG, M. C. & SANFORD, T. B. 1980 Signatures of mixing from the Bermuda Slope, the Sargasso Sea and the Gulf Stream. *J. Phys. Oceanogr.* **10**, 105–127.

HESKESTAD, G. 1965 A generalized Taylor hypothesis with application for high Reynolds number turbulent shear flows. *Trans. ASME* E: *J. Appl. Mech.* **87**, 735–740.

HILL, R. J. 1978 Models of the scalar spectrum for turbulent advection. *J. Fluid Mech.* **88**, 541–562.

HOLLOWAY, G. & KRISTMANNSSON, S. S. 1984 Stirring and transport of tracer fields by geostrophic turbulence. *J. Fluid Mech.* **141**, 37–50.

KAIMAL, J. C., WYNGAARD, J. C., IZUMI, Y. & COTÉ, O. R. 1972 Spectral characteristics of surface-layer turbulence. *Q. J. R. Met. Soc.* **98**, 563–589.

KRAICHNAN, R. H. 1968 Small-scale structure of a scalar field convected by turbulence. *Phys. Fluids* **11**, 945–953.

KOLMOGOROFF, A. N. 1941 The local structure of turbulence in an incompressible viscous fluid for very large Reynolds number. *C.R. Acad. Sci. USSR* **30**, 301–305.

KOLMOGOROFF, A. N. 1962 A refinement of previous hypotheses concerning the local structure of turbulence in a viscous incompressible fluid at high Reynolds number. *J. Fluid Mech.* **13**, 82–85.

LANGE, R. E. 1982 An experimental study of turbulence behind towed biplanar grids in a salt-stratified fluid. *J. Phys. Oceanogr.* **12**, 1506–1513.

LESIEUR, M. & HERRING, J. 1985 Diffusion of a passive scalar in two-dimensional turbulence. *J. Fluid Mech.* Submitted.

LUMLEY, J. L. 1965 Interpretation of time spectra measured in high intensity shear flows. *Phys. Fluids* **8**, 1056–1062.

MESTAYER, P. 1982 Local isotropy in a high-Reynolds-number turbulent boundary layer. *J. Fluid Mech.* **125**, 475–503.

MONIN, A. S. & YAGLOM, A. M. 1975 *Statistical Fluid Mechanics*, Vol. 2. MIT Press. 874 pp.

OAKEY, N. S. 1982 Determination of the rate of dissipation of turbulent energy from simultaneous temperature and velocity shear microstructure measurements. *J. Phys. Oceanogr.* **12**, 256–271.

OBOUKOV, A. M. 1949 Structure of the temperature field in a turbulent flow. *Izv. Akad. Nauk SSSR Ser. Geogr. i Geofiz.* **13**, 58–69.

OBOUKOV, A. M. 1962 Some specific features of atmospheric turbulence. *J. Fluid Mech.* **13**, 77–81.

OZMIDOV, R. V. 1965 On the turbulent exchange in a stably stratified ocean. *Izv. Atmos. & Oceanic Phys. Ser.* **1**, 853–860.

PAQUIN, J. E. & POND, S. 1971 The determination of the Kolmogoroff constants of velocity, temperature and humidity fluctuations from second- and third-order structure functions. *J. Fluid Mech.* **50**, 257–269.

PHILLIPS, O. M. 1977 *The Dynamics of the Upper Ocean*, 2nd Edn. Cambridge University Press. 336 pp.

SCHMITT, K. F., FRIEHE, C. A. & GIBSON, C. H. 1978 Humidity sensitivity of atmospheric temperature sensors by salt contamination. *J. Phys. Oceanogr.* **8**, 151–161.

STEWART, R. W. 1969 Turbulence and waves in a stratified atmosphere. *Radio Sci.* **4**, 1269–1278.

STILLINGER, D. C., HELLAND, K. N. & VAN ATTA, C. W. 1983 Experiments on the transition of homogeneous turbulence to internal waves in a stratified fluid. *J. Fluid Mech.* **131**, 91–122.

TENNEKES, H. & LUMLEY, J. L. 1972 *A First Course in Turbulence.* MIT Press. 300 pp.

VAN ATTA, C. W. 1971 Influence of fluctuations in local dissipation rates on turbulent scalar characteristics in the inertial subrange. *Phys. Fluids* **14**, 1803–1804.

VAN ATTA, C. W. 1973 Erratum: Influence of fluctuations in local dissipation rates on turbulent scalar characteristics of the inertial subrange. *Phys. Fluids* **16**, 574.

WEILER, H. S. & BURLING, R. W. 1967 Direct measurements of stress and spectra of turbulence in the boundary layer over the sea. *J. Atmos. Sci.* **24**, 653–664.

WILLIAMS, R. M. & PAULSON, C. A. 1977 Microscale temperature and velocity spectra in the atmospheric boundary layer. *J. Fluid Mech.* **83**, 547–567.

WYNGAARD, J. C. & PAO, Y. H. 1971 Some measurements of the fine structure of large Reynolds number turbulence. In *Statistical Models and Turbulence* (ed. M. Rosenblatt & C. Van Atta). Lecture Notes in Physics vol. 12, Springer.

YAGLOM, A. M. 1966 The influence of fluctuations in energy dissipation on the shape of turbulence characteristics in the inertial interval. *Sov. Phys. Dokl.* **11**, 26.